Nasa CR-65420

THE Marquardt CORPORATION VAN NUYS, CALIFORNIA

MR 3008-F

MATERIALS REPORT

for

APOLLO SERVICE MODULE

REACTION CONTROL SYSTEM ENGINE

CHAMBER SEAL STUDY

PREPARED UNDER CONTRACT NAS 9-4775

TMC 3008

[redacted]

Prepared by J. Puntar
J. Puntar
Principal Investigator

Approved by E. P. Perlman
E. P. Perlman
Program Manager

GPO PRICE $

CFSTI PRICE(S) $

Hard copy (HC) 3.00

Microfiche (MF) .75

ff 653 July 65

[redacted]

[illegible]

[illegible]

TABLE OF CONTENTS

I. INTRODUCTION AND SUMMARY

This report, submitted in final fulfillment of Part VIII, Contract NAS 9-4775, summarizes the technical data obtained in tests and experimental activities relating to materials used in fulfilling the requirements of the subject contract. Metallic and non-metallic materials with low thermal conductivities and high strength were evaluated in conjunction with the development of high thermal resistance injector head/combustion chamber seals for the Apollo Service Module Reaction Control System (S/M RCS) engine.

II. DISCUSSION

A total of three (3) metallic materials were tested to determine specific structural properties and failure modes as applied to seals developed in the Chamber Seal Study Program. The materials were:

1. 6AL-4V, Titanium Alloy
2. Rene' 41
3. L-605, Cobalt Base Alloy (20% cold worked)

Objectives of the tests on these metals were to:

A. Determine compressive/bearing strength of these materials in combination with disilicide coated, unalloyed Molybdenum.

B. Determine bearing strength of the disilicide coated Molybdenum in combination with these materials.

C. Identify the compressive/bearing failure mode of these materials in combination with the disilicide coated Molybdenum.

Room temperature tests indicated that:

FOR YIELD - Bearing stresses, corresponding to Molybdenum material deformations of .0001 to .0002 inch, ranged at an average 200 ksi.

FOR ULTIMATE - Bearing stresses, corresponding to Molybdenum material deformations of .0006 to .0015 inch, ranged from 215 ksi to 222 ksi.

FAILURE MODE - The metallic specimens and the disilicide coated and lapped Molybdenum material exhibited clean perceptable local yielding at the highly stressed areas.

In addition to the three metallics, three (3) non-metallics were also tested. These materials were the following grades of Zirconium Oxide:

4. Zircoa "C" (full dense) - 347 lbs/ft^3
5. Zircoa "C" (modified) - 269 lbs/ft^3
6. Zircoa 1027 (modified) - 275 lbs/ft^3

Objectives of the tests on the non-metallics were to:

A. Verify the ultimate compressive strength of these materials in combination with the candidate metals.

B. Evaluate their behavior under static load in combination with the candidate metals.

The tests, conducted at room temperature, indicated that the ultimate compressive strength of the three materials was:

ZIRCOA "C" (full dense) - 130 ksi to 148 ksi

ZIRCOA 1027 (modified) - 110 ksi to 115 ksi

ZIRCOA "C" (modified) - 83.5 ksi to 97.5 ksi

A detailed discussion of the tests, summarized above, is presented in Exhibit A which was extracted from the Marquardt Program Final Report PR 3008-F, dated June 1966.

Additional technical data, relative to the thermal properties (viz., thermal conductivity) of the non-metallics discussed above, are also included in Exhibit A.

EXHIBIT A

Excerpts from Final Report PR 3008-F relating to materials used in fulfilling the requirements of Contract No. NAS 9-4775.

THE Marquardt CORPORATION VAN NUYS, CALIFORNIA

TEST REPORT (FINAL)

SMALL SCALE MATERIAL SPECIMENS

FOR

APOLLO SERVICE MODULE

REACTION CONTROL SYSTEM ENGINE INJECTOR

CHAMBER SEAL STUDY

PREPARED UNDER CONTRACT NAS 9-4775

TMC 3008

Prepared By J. Puntar
J. Puntar
Design Engineering

Approved By E. P. Perlman
E. P. Perlman
Program Manager

TABLE OF CONTENTS

LIST OF ILLUSTRATIONS

T A B L E O F C O N T E N T S (Continued)

TABLE OF CONTENTS (Continued)

I. INTRODUCTION

This test report covers the results in testing candidate seal materials in support of development of high thermal resistance injector head/combustor seals for the Apollo Service Module Reaction Control System Engine under Contract NAS 9-4775. Metallic and non-metallic small scale specimens fabricated from candidate seal materials were tested to determine specific structural properties and failure modes as applied to seals developed in this program.

II. CONCLUSIONS AND RECOMMENDATIONS

Analysis of test data obtained from small scale metallic specimen structural tests indicated that sufficient safety margins were attained with these materials in combination with the disilicide coated molybdenum combustion chamber material. The materials tested, 6AL-4V Titanium Rene' 41 and L-605, were proven to be suitable engineering materials for high thermal resistance seals.

Non-metallic specimens, fabricated from two (2) different types of Zirconium Oxide, demonstrated compressive strengths commensurate with requirements for composite type seals. Structural safety margins in excess of maximum ultimate stress (Apollo specifications define this as "maximum limit stress" x 1.5) were documented. A third type of Zirconium Oxide demonstrated compressive strength equivalent to 78% of the required value.

On the basis of static compression tests, Zirconium Oxide material is suitable for application to composite type high thermal resistance seals.

III. SUMMARY

Small scale bearing tests of specimens fabricated from candidate seal metals were conducted. Test data indicated that sufficient safety margins in bearing were attained with these materials in combination with the disilicide coated molybdenum combustor flange. A summary of the test results follows:

RESULTS OF SMALL SCALE BEARING TESTS - SUMMARY

Small scale specimens fabricated from 6AL-4V Titanium, Rene' 41 and 20% cold worked L-605 cobalt base alloy, in combination with a disilicide coated and lapped molybdenum combustor flange used in the Apollo SM RCS Engine were subjected to bearing loads induced by the Baldwin Universal Compression Test Machine. Each specimen contained a contact bearing width of .017/.019 inch corresponding to the bearing width on the straight thinwall seal at the seal/combustor interface. Load steps were applied serially at room temperature to individual specimens to establish the bearing strength of the coated flange.

A yield criteria at bearing stresses corresponding to moly flange deformations of .0001 to .0002 was chosen. For these deformations, which correspond to an average 270 lbs. loss of seal preload, the minimum bearing stress was 154,000 psi and the maximum was 200,000 psi. The yield allowable of 166,000 psi used in SM 153, Stress Analysis of Seal Configurations (Ref. 1), would seem to be justified.

The ultimate criteria was taken to be that stress corresponding to the maximum observed permanent deformations, .0006 and .0015 inch. For these deformations, which correspond to an average loss of 1800 lbs. seal preload, the minimum bearing stress was 215,000 psi and the maximum 222,000 psi. These values are higher than those used in the seal stress analysis which was 183,700 psi at 150°F.

Failure mode of the specimens and the molybdenum disilicide coated and lapped molybdenum combustor flange was manifested by clean perceptable local yielding at the highly stressed areas.

Tests verifying the compressive strength of three (3) different types of Zirconium Oxide in combination with candidate seal metals were conducted. Problems were experienced initially in obtaining consistent test data.

A summary of test results follows:

<u>RESULTS OF SMALL SCALE ZIRCONIUM OXIDE COMPRESSION TESTS - SUMMARY</u>

Small scale specimens, .050/.051 diameter x .053/.054" long, full dense, hard fired Zirconium Oxide (Zircoa "C") in combination with candidate seal metals were subjected to oompressive loads generated by the Baldwin Universal Compression Test Machine. Loading was applied at a low strain rate at room temperature to individual specimens aimed at establishing the compressive strength of the Zirconium Oxide.

Favorable test results were obtained on five (5) specimens load tested to levels exceeding the required minimum without failure. Stresses ranging between 112.5 to 140 ksi were demonstrated. The required ultimate compressive strength is 112.95 ksi.

Additional specimens of the same material were also fabricated and tested using .080 inch and .250 inch diameters with a length to diameter ratio of unity. These tests were aimed at establishing compressive strength corresponding to failure.

Two (2) specimens of each size were individually load tested to apparent failure using the same test method. Erratic test results were obtained. Failure stresses ranging from 33 to 95.2 ksi were recorded. It was concluded that uneven specimen loading resulting in deviation from ideal test conditions was caused by minute, unobservable shifts within the test setup. No further attempts were made to obtain F_{c_u} values for this material using the singular specimen test method.

Another test, however, was designed and implemented which was very successful in attaining consistent compression test data of a more practical nature. The test method employed three (3) .050/.051 x .053/ .054" long specimens nested equidistantly within a composite seal jacket. In this case, it was predicted that one of the three specimens would fail upon reaching it's discrete critical stress. In practice, the failure point was realized by an instantaneous collapse of the weakest specimen.

Three (3) different types of Zirconium Oxide materials were tested on the Baldwin Compression Test Machine using this method, Zircoa "C" (full dense), Zircoa "C" (modified) and Zircoa #1027 (modified) were fabricated into test specimens. The first material previously discussed, was selected early in the program while the latter two were specially developed later in the program. The modified materials were aimed at obtaining lower thermal conductivity (K) consistent with high compressive strength.

Uniform test results were obtained from three (3) "triplet" sets (consisting of three cylinders/set) for each material. Failure stresses ranging from 130 to 148 ksi were recorded for the Zircoa "C" (full dense) material, 110 to 115 ksi for the Zircoa #1027 (modified) material and 83.5 to 97.5 ksi for the Zircoa "C" (modified) material.

Compression load tests were also performed on "ganged" Zirconium Oxide cylinders. This testing was facilitated by assembling sixty (60) cylinders into composite seal jackets. Four (4) assemblies conforming to full scale composite seal assemblies P/N T-13618 (Titanium jacket seal) and P/N T-13619 Rene' 41 jacket seal) were load tested. No failures or indications of structural degradation were observed after application of 5880 lbs. compressive load was applied by the Baldwin Universal Compression Test Machine. (5880 lbs. load corresponds to the maximum preload applied to seals during Apollo engine assembly).

IV. TECHNICAL DISCUSSION AND TEST RESULTS

Small scale specimen testing of candidate seal materials was performed at the Marquardt Materials and Process Laboratory. Informal test outlines were used in lieu of formal test plans in order to facilitate the flexibility in changes to test setups and test procedures.

Early in this program, four (4) candidate materials were chosen as best suited for high thermal resistance seals. They are:

1. 6AL-4V, Titanium alloy
2. Rene' 41
3. L-605, cobalt base alloy (20% cold worked)
4. Zirconium Oxide (Zircoa "C")

Small scale specimens were fabricated from the metallic materials and subjected to compression tests on the Baldwin Universal Compression Test Machine. The metallic specimens:

1. 6AL-4V
2. Rene' 41
3. L-605

were designed to contain a contact bearing width of .017/.019 inch. Corresponding to that reflected by the straight thinwall seal designs (P/N's T-13611 and T-13612) at the seal/combustor interface. Bearing widths on conical thinwall and composite seals are larger and less critical, therefore, were not tested in small scale.

An Apollo production combustor fabricated from un-alloyed molybdenum was obtained from the Apollo project. The combustor was disilicide coated and the flange face (adjacent to the seal) was lapped per Apollo specifications.

Objectives of the tests were to verify contact bearing width requirements analytically estimated for the thinwall seal at the combustor interface. Additionally, the bearing strength of the combustor flange was to be determined as well as identification of the compressive/bearing failure modes of the candidate metals in combination with the combustor flange.

Early tests were conducted on specimens with small contact bearing widths (.015/.017 inch). A design change to the thinwall seals (contact bearing width was increased to .017/.019), coupled with test setup instability problems, terminated testing of these specimens. A description of the specimens and test setup is shown in Figure 1.

Figure 2 describes the revised specimens and test setup. The test procedure consisted of applying load steps, at room temperature, to individual specimens. Load steps are tabulated in Figure 3. After each load step, the loading was removed and a visual inspection was made of the specimen and combustor flange surface for indications of changes (brinelling and/or deformations). Succeeding load steps were made at new locations on the flange. At the conclusion of load step application, all positions were measured to record minimum and maximum depths of impressions on the flange surface. An indicator with .00005 inch accuracy was used. Each specimen was also measured to obtain bearing areas at the specimen/combustor flange interface and the stresses corresponding to each load step were calculated.

Figure 4 tabulates the deformation measurements, bearing areas and stresses for all specimens at each load step.

Figure 5 is a cross plot of the moly flange bearing stress vs. indentation taken from Figure 4.

Analysis of these data resulted in choosing yield criteria at bearing stresses corresponding to moly flange deformations of .0001 to .0002. The plot (Figure 5) shows one data point at 154 ksi at .00015 inch indentation with all others at an average of 200 ksi. The yield allowable of 166,000 psi used in (Ref. 1), SM 153, Stress Analysis of Seal Configurations, would seem to be justified.

For ultimate criteria, permanent deformations of .0006 to .0015 inch were chosen. The plot (Figure 5) shows bearing stresses ranging from 215 ksi to 222 ksi. These values are higher than 183,700 psi used in Ref. 1.

Compression testing of non-metallic specimens was completed for three (3) different types of Zirconium Oxide. The primary variable for the three (3) types of materials is bulk density (lbs/ft^3). The materials and bulk densities are:

1. Zircoa "C" (full dense) - 347 lbs/ft^3
2. Zircoa "C" (modified) - 269 lbs/ft^3
3. Zircoa #1027 (modified) - 275 lbs/ft^3

Chemically, materials 1 and 2 are identical. The third material consists primarily of Zirconia. The other constituants in this material are considered proprietary by the manufacturer, Zirconium Corporation of America, thus, could not be obtained.

Initially, small scale specimens were fabricated from Zircoa "C" rod. This material was chosen early in the program for it's high compressive strength and low thermal conductivity. It is described as dense, hardfired, lime stabilized Zirconium Oxide.

The specimens used in the first test series conformed to dimensional requirements of Drawing T-13617 (.050/.051 diameter x .053/.054 inch long).

Objectives of the tests were to verify the compressive strength of the material and evaluate its' behavior under load in combination with candidate seal metals.

Initial tests produced erratic test results. The variance in test results was primarily due to uneven specimen loading manifested by the test setup and test procedures used. The test setup is illustrated in Figure 6. The test procedure consisted of applying load steps at room temperature similar to the procedure used for metallic specimens.

Reasons for the erratic performance is explained as follows:

> Zirconium Oxide, having a crystalline structure consistent with a relatively high modulus of elasticity (ϵ = 21.5 x 10 psi @ R.T.), is a brittle material with reportedly very high compressive strength (F_{cu} = 303,000 psi @ R.T. under ideal loading conditions). The ultimate

tensile strength, however, is relatively low (F_{tu} = 20,000 psi). To obtain absolute F_{cu} values, even specimen loading, applied at a low strain rate is essential to maintain a compressive mode uniformly within the material. Should uneven loading be applied across the specimen, a shear mode can be generated in the material resulting in a tensile failure at the shear plane.

The test setup was modified, as shown in Figure 7. The modification consisted of providing a "centering nest" for the specimens to obviate articulation of the test setup elements under load. The nest was designed to accommodate a single specimen or three specimens arranged in a circular pattern, evenly spaced about the load axis.

The revised test procedure consisted of applying a continuously increasing load at a low strain rate instead of interrupted load steps.

Five (5) specimens were tested individually in accordance with the above. Favorable results were obtained on all specimens. Results are compared with required performance as follows:

Specimen No. (.050/.051 Dia. x .053/.054 In. Lg.)	Applied Load-Lbs. (2-3 Lbs/Sec.)	Demonstrated Equiv. Compressive Stress-Psi x 10^3	Required Ult. Comp. Strength -Psi x 10^3
#1	270*	135	↑
#3	280*	140	
#4	260*	130	112.95**
#5	275*	137.5	
#6	225*	112.5	↓

*Load applied at constant rate to value shown - no failure.

**Maximum Apollo launch boost limit σ x M.S. (1.5) = Maximum Ult. σ = (75.3 x 1.5) x 10^3 for individual cylinder.

Photographs taken of each end of the tested specimens, Figure 8, indicate that minor degradation of the edges is evident. This was expected due to edge loading effects. However, the resultant loss of cross sectional area at the specimen faces combined with the ability of the remaining material to sustain the applied load, indicates that the material was capable, in each case, of bearing additional load. Loading, however, was purposely stopped at the values shown to permit inspection of the specimens prior to failure.

Additional tests were conducted on specimens made from the same material to establish compressive strength corresponding to failure.

Cylindrical specimens, .080 inch and .250 inch diameter with a length to diameter ratio of unity were tried. The outside diameters of these specimens were "unground", i.e., in the "as fired" condition to preserve the fired skin and obviate the presence of grinding cracks which might contribute to premature failure. Presence of these cracks, if they in fact exist, has never been detected on any parts fabricated from zirconia in this program. Faces of the specimens were ground flat and parallel. The test setup, shown in Figure 9, employed a RTV rubber cast to nest a single specimen properly between the metallic slugs. A continuously increasing load at a low rate was applied by the Baldwin Universal compression test machine. At approximately fifty (50) lbs. load, the RTV nest, which was previously slitted, was removed (to permit viewing the specimen) while the load was continuously increased (without interruption) until failure was detected. Failure detection was facilitated by simultaneous observation of the specimen and the Baldwin load gauge. Load application was terminated when either the specimen showed signs of failing or the load gauge showed erratic load rate steps. Two (2) specimens of each size (.080 inch diameter and .250 inch diameter) were tested with erratic test results. Figure 10 summarizes these results. Figure 11 documents the pre and post test condition of the .080 inch diameter specimens. Figure 12 shows the pre and post test condition of the .250 inch diameter specimens. Although the photographs do not indicate total failure of all the cylinders, it is believed that visually undetectable cracks within the material were responsible for the erratic load rate steps observed on the Baldwin load gauge. It was concluded that minute, unobservable shifts within the test setup caused uneven specimen loading and deviation from ideal test conditions. No further attempts were made to obtain, the hoped for, absolute F_{cu} values for this material.

Another test, however, was designed and implemented which was very successful in attaining consistent test data of a more practical nature. This test employed three (3) standard size zirconia cylinders, fabricated per Drawing T-13617, and the titanium jacket and bumperset, P/N's T-13614 and T-13615, previously used in a thermal test. The three (3) cylinders were nested equidistantly within the jacket by the bumper set. The snapring was purposely not used in order to permit visual access to the cylinders. The setup, shown in Figure 13, also used the simulated injector head (from thermal tests), moly combustor ring (from small scale metallic specimen tests) and a molybdenum simulated combustor. Compressive loads were applied at a low rate by the Baldwin compression test machine. The accurate geometry of the test setup elements and small L/D ratio described by the test setup extremities assured equal load distribution to each cylinder consistent with excellent stability. Further, the setup provided accurate simulation of uneven loading conditions which prevail at the cylinder/jacket interfaces in the composite seal.

The test procedure employed the same failure detection methods used in the single specimen tests, i.e., simultaneous observation of the specimens and the Baldwin load gauge. In this case, it was predicted that one of the three specimens would fail upon reaching it's discrete critical stress. In practice, the failure point was realized by an instantaneous collapse of the weakest specimen which was recorded accurately by the Baldwin load gage.

All three (3) different types of Zirconium Oxide materials were successfully tested on the Baldwin compression test machine using this test method to determine the ultimate compressive strengths corresponding to failure.

Uniform test results were obtained from all three (3) "triplet sets" (consisting of 3 cylinders/set) for each material. A comparison of the test results is shown in Figure 14. The data is considered to be reliable as well as practical in that it was generated under typical loading conditions as found normally in composite seals.

Figures 15 through 23 document the pre and post-test condition of each triplet set. The post-test photographs show the characteristic minor edge degradation (on each of the unfailed specimens) which prevails due to edge loading effects. This type of edge degradation does not occur at stresses corresponding to limit loads.

Load tests were also performed on completely assembled composite seals. Both composite configurations, P/N's T-13618 (Titanium) and T-13619 (Rene' 41) were subjected to approximately three (3) ton (5880 lbs.) loads in the Baldwin Universal Compression Test Machine. No failures or indications of structural degradation occurred. The 5880 lbs. load is equivalent to the maximum preload applied during Apollo engine assembly. These tests (regarded as acceptance tests for composite seals) confirmed the suitability of composite seal jackets which contained minor distortions. These seals were subsequently reloaded successfully by the standard Apollo assembly techniques (with combustor attach bolts) in the structural and thermal test rigs.

The test setup for the assembled composite seals is shown in Figure 24.

REFERENCES:

1. Stress Memo - SM 153, Stress Analysis of Seal Configurations - G. Carayanis

BEARING TEST SETUP & SPECIMENS

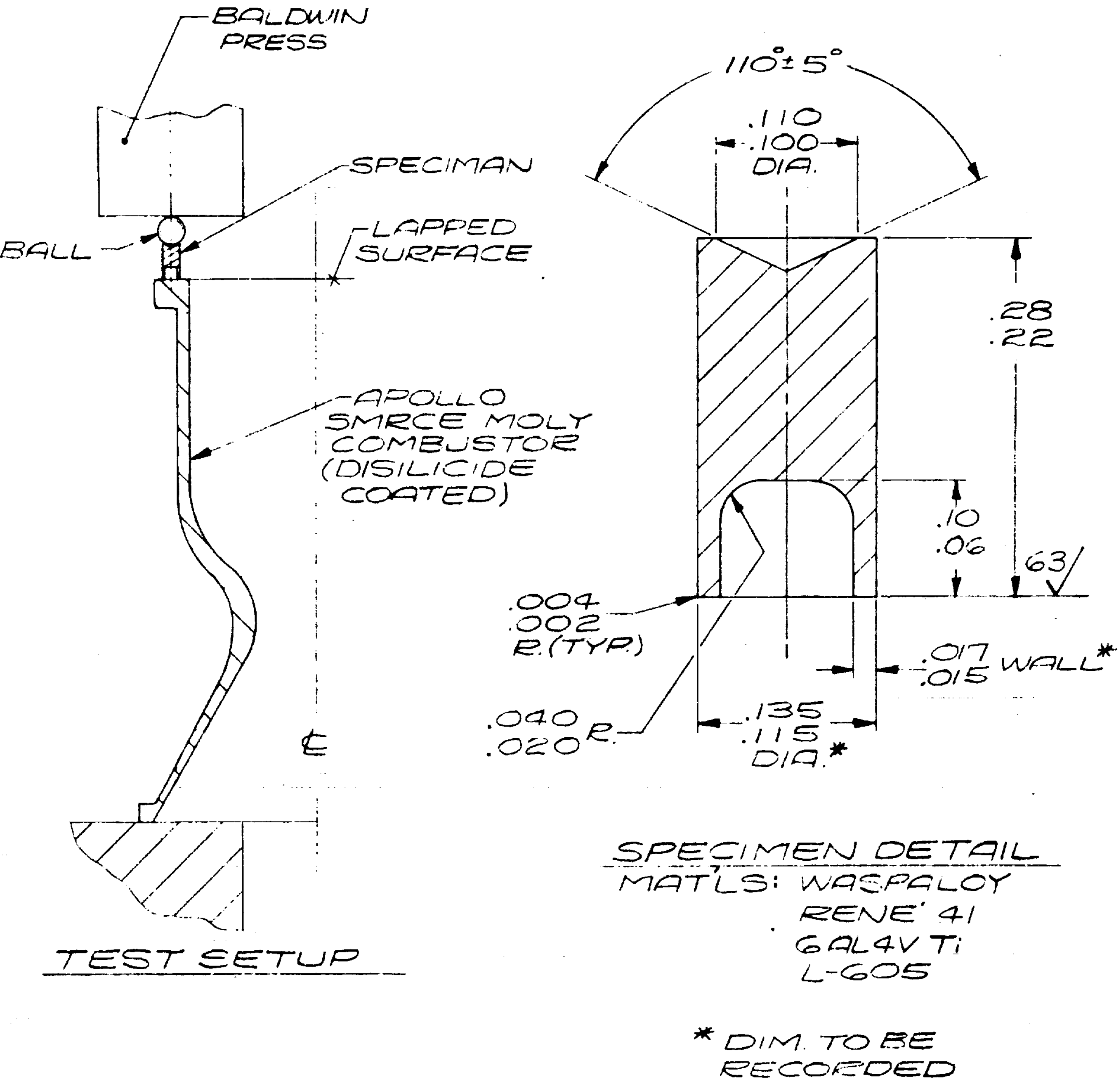

FIGURE 1

BEARING TEST SETUP & SPECIMENS

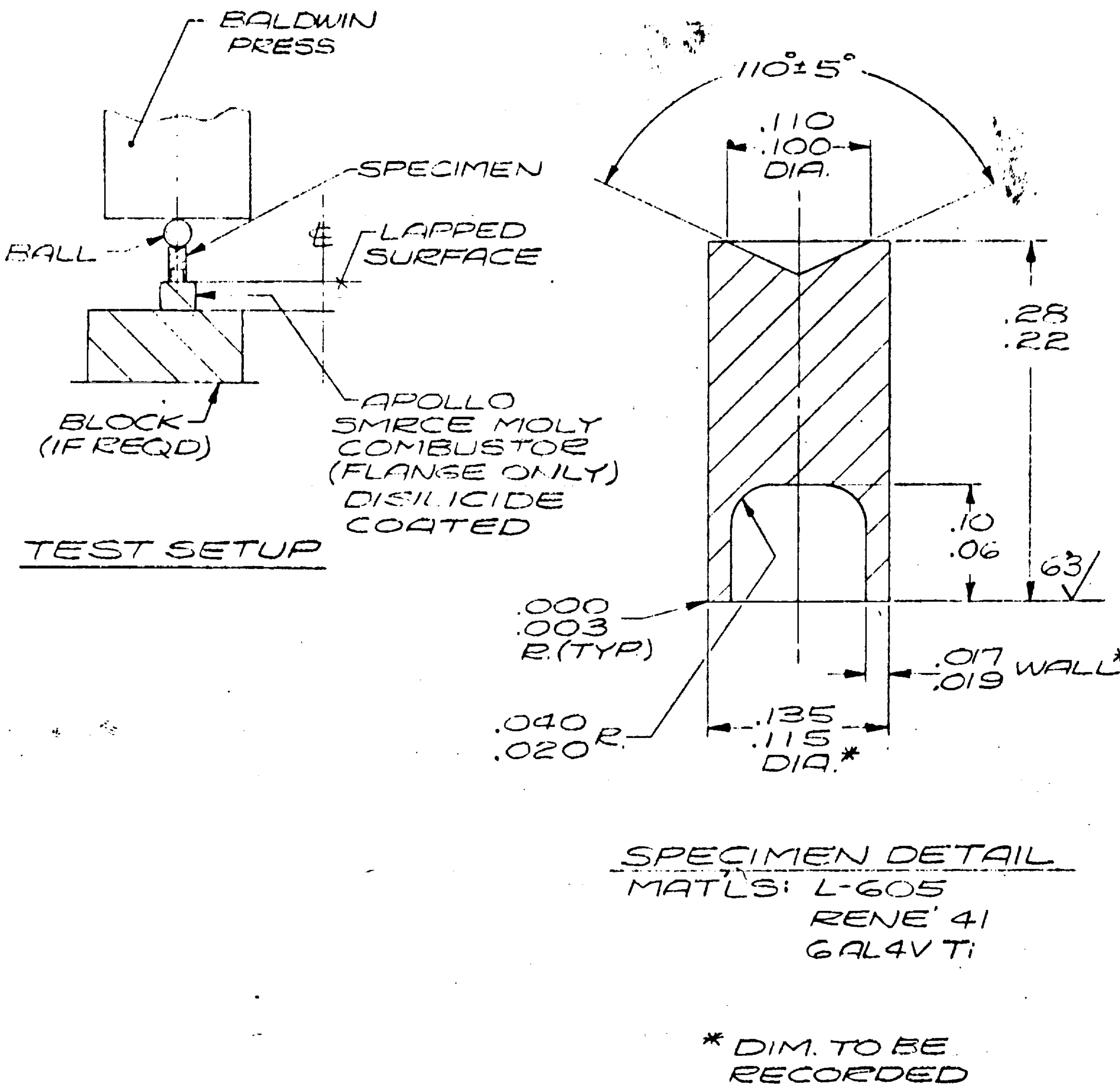

FIGURE 2

LOAD STEPS - SMALL SCALE SPECIMENS,
CANDIDATE SEAL METALS

Load Steps	L-605	Rene' 41	6AL-4V Ti
1	370#	830#	860#
2	460#	1040#	1080#
3	560#	1250#	1300#
4	650#	1460#	1510#
5	740#	1660#	1720#

FIGURE 3

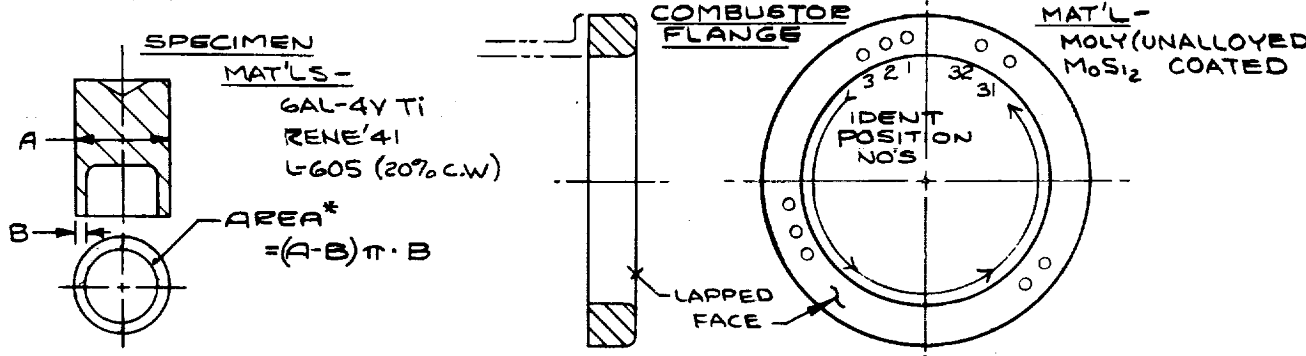

TABULATION - LOAD & STRESS DATA

	POS. NO.	INDENTATION (IN×10⁻⁴) MIN.	MAX.	LOAD (LBS.)	A-B (IN.)	B (IN.)	AREA* (IN²×10⁻³)	σ (KSI)	IDENT. AVG.(IN×10⁻⁴)
L-605	1	0	0	560	.1064	.017	5.68	98.6	0
	2	0	0	650	NOT RECORDED		/	/	/
	3	0	0	740	NOT RECORDED		/	/	/
	4	0	0.6	1,100	.1058	.018	5.98	183.9	0.3
	5	6.0	15.0	1,500	.1170	.019	6.98	214.8	10.5
RENE 41	6	1.0	2.0	840	.1083	.016	5.44	154.4	1.5
	7	2.0	3.0	1,040	NOT RECORDED		/	/	/
	8	1.0	5.0	1,250	.1088	.017	5.81	215.1	3.0
	9	4.0	7.0	1,400	.1114	.018	6.30	222.2	5.5
Ti	10	0	1.0	1,080	.1051	.019	6.27	172.2	0.5
	11	2.0	4.0	1,300	.1057	.0195	6.47	200.9	3.0
	12	1.0	1.0	1,400	.112	.020	7.04	198.9	1.0
L-605	13	1.0	3.0	1,100	.1052	.018	5.95	184.8	2.0
	14	3.0	4.0	1,250	.1054	.018	5.96	209.7	3.5
	15	2.0	3.0	1,400	.1061	.0185	6.16	227.3	2.5
	16	1.0	4.0	1,500	.1098	.0195	6.72	223.2	2.5
RENE 41	17	0	0	1,040	.1077	.017	5.75	180.8	0
	18	1.0	2.0	1,250	.1080	.018	6.11	204.8	1.5
	19	1.5	2.0	1,400	.1142	.018	6.46	216.7	1.75
Ti	20	0	1.0	1,080	.1082	.0175	5.95	181.5	0.5
	21	0	5.0	1,300	.1090	.018	6.16	211.0	2.5
	22	1.0	4.0	1,460	.1170	.020	7.35	198.6	2.5
L-605	23	0.5	1.0	1,100	.1066	.019	6.36	173.0	0.75
	24	0	1.0	1,250	.1063	.019	6.34	197.2	0.5
	25	1.0	1.5	1,400	.1076	.019	6.42	218.1	1.25
	26	0	1.0	1,500	.1118	.019	6.67	224.9	0.5
RENE 41	27	1.0	2.0	1,040	.1087	.017	5.80	179.3	1.5
	28	1.0	3.0	1,250	.1097	.017	5.86	213.3	2.0
	29	1.5	3.0	1,430	.1115	.0175	6.13	233.3	2.25
Ti	30	0	0	1,080	.1073	.018	6.07	177.9	0
	31	0	1.5	1,300	.1078	.018	6.09	213.5	0.75
	32	1.0	2.0	1,410	.1110	.019	6.62	213.0	1.5

FIGURE 4

MOLYBDENUM CHAMBER BEARING STRESS VS. INDENTATION

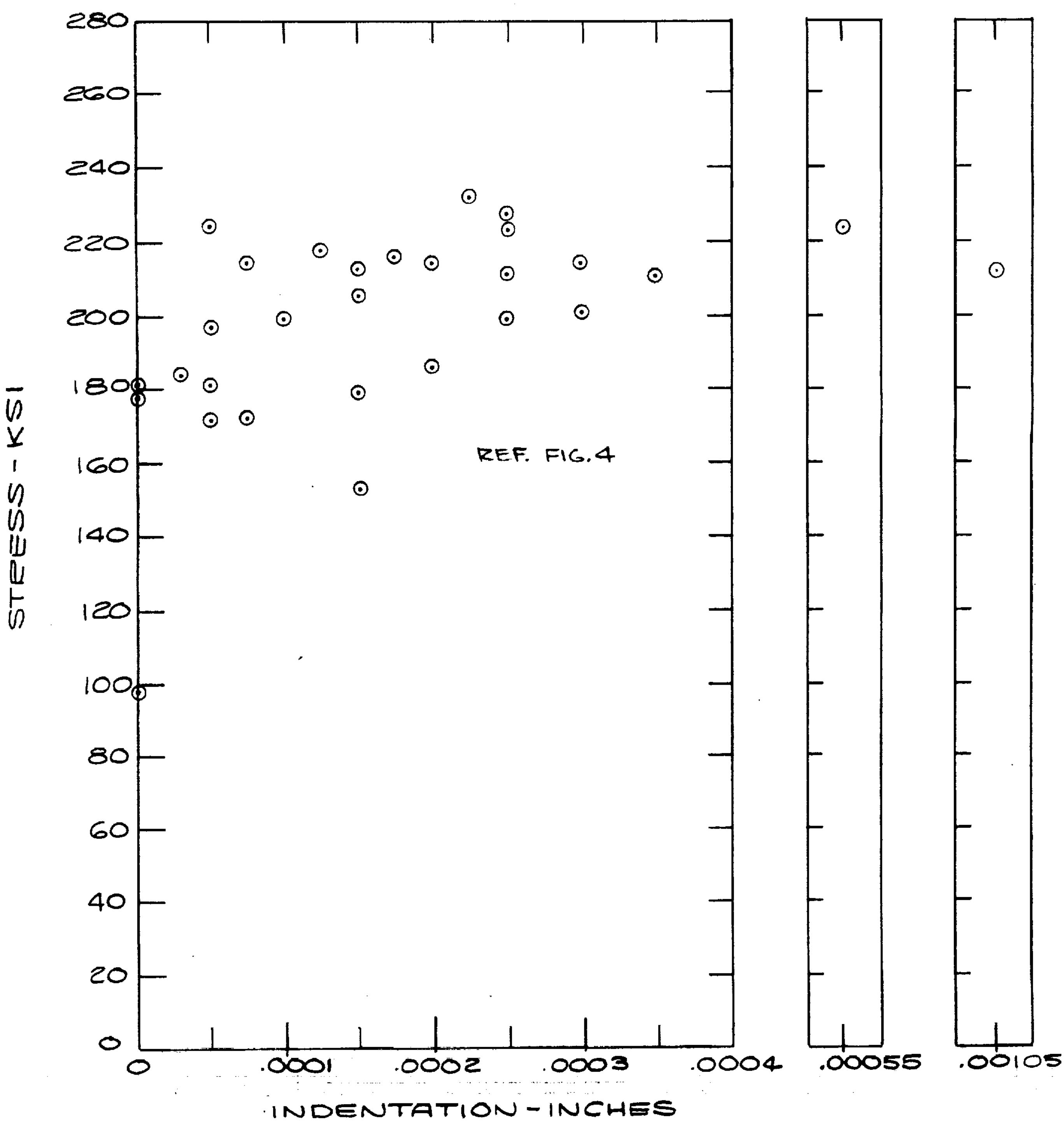

FIGURE 5

TEST SETUP

COMPRESSION TEST - ZIRCOA "C" VS. CANDIDATE METALS

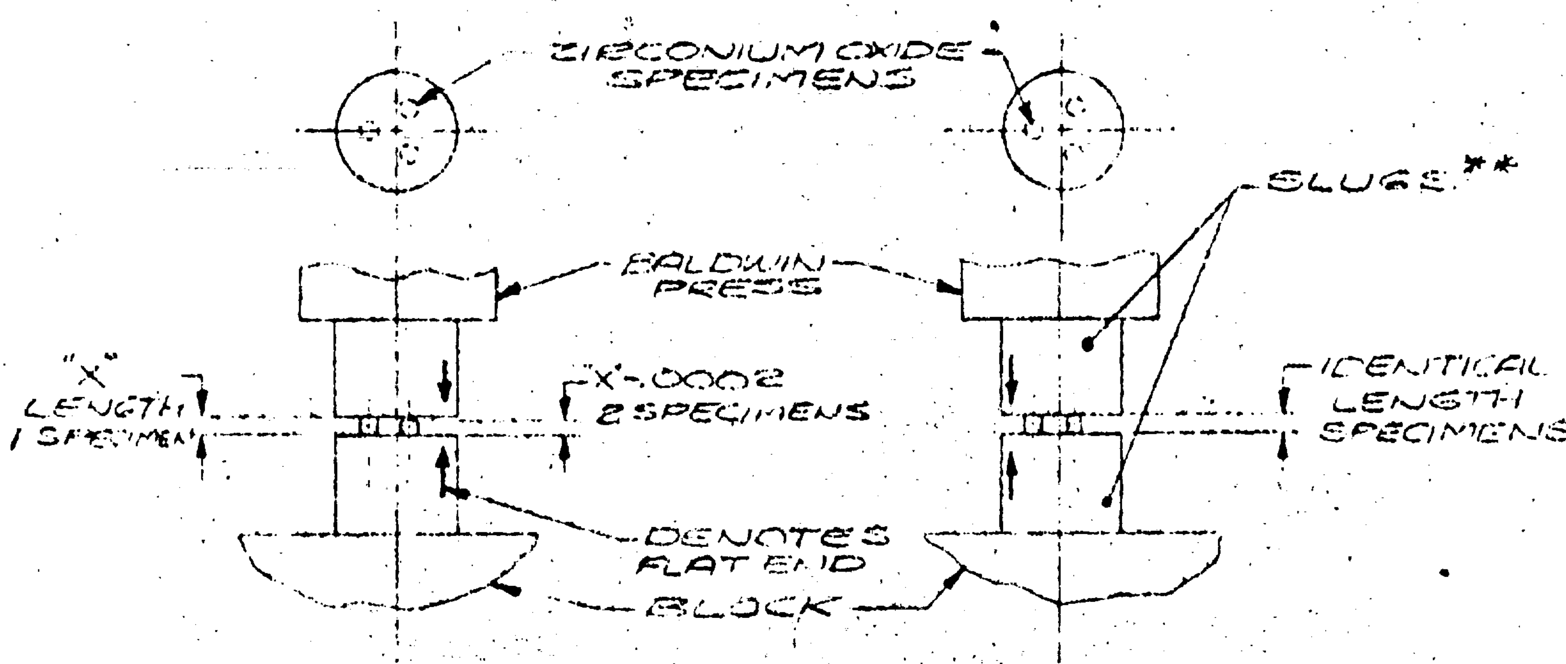

SETUP #1 SETUP #2

** MAT'L
1. L-605
2. RENE 41
3. 6AL-4V TI

TEST PROCEDURE

1. USING L-605 SLUGS IN SETUP #1 APPLY LOADS PER TABLE I. INSPECT PARTS BETWEEN LOAD STEPS.
2. REPEAT STEP 1 WITH SLUGS OF RENE 41, 6AL-4V TI & NEW ZIRCONIUM OXIDE SPECIMENS.
3. USING TEST SETUP #2, USE PROCEDURE PER STEPS 1 & 2.

TABLE I

LOAD STEPS	1	2	3	4	5	6	7	8	9	10
LOAD (LBS)	200	300	400	600	800	1000	1200	1400	1600	1800

FIGURE 6

TEST SETUP
COMPRESSION TEST - ZIRCOA "C" VS. CANDIDATE METALS

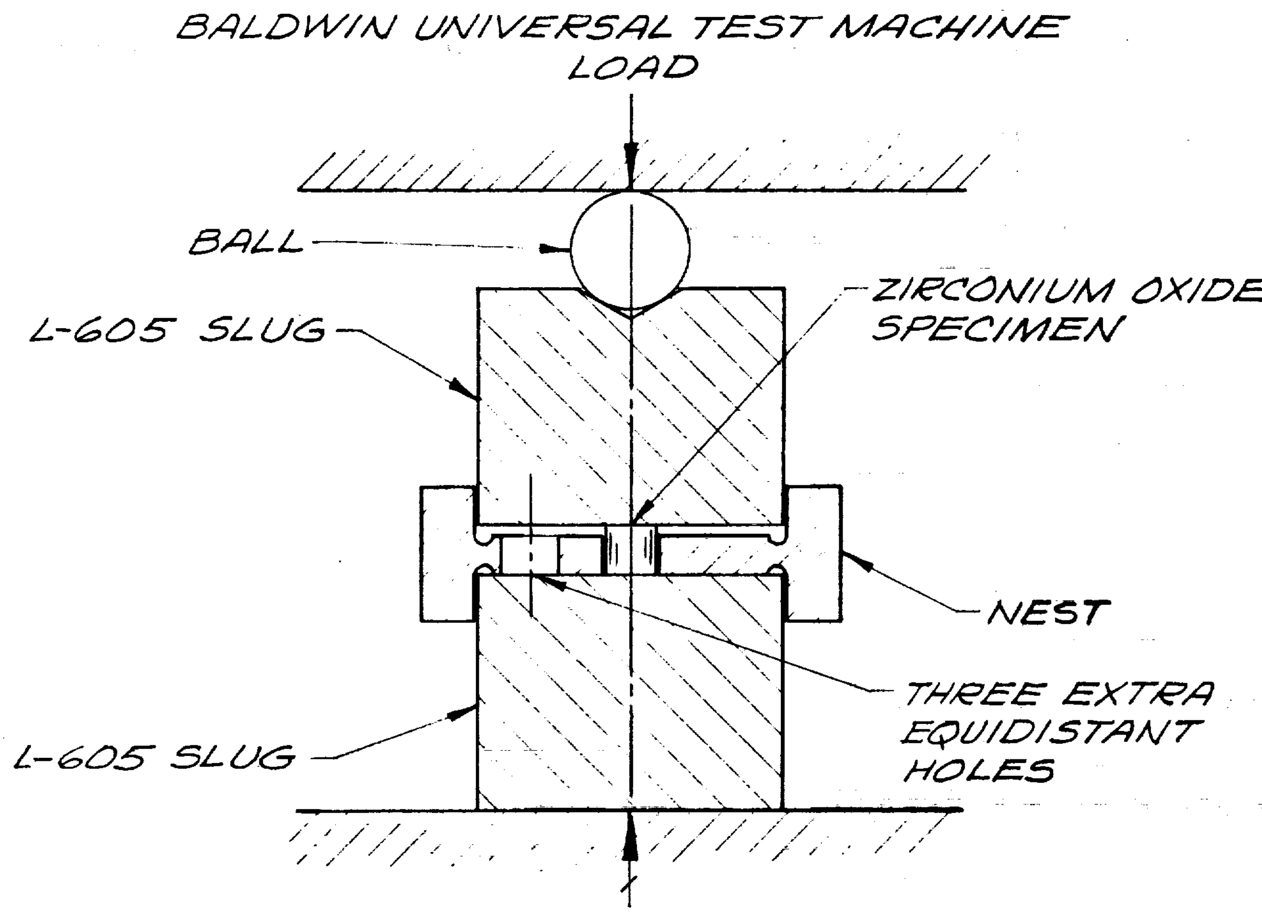

5/1 SCALE

FIGURE 7

ZIRCOA 'C' (ZIRCONIUM OXIDE) COMPRESSION TEST SPECIMENS
.053/.054 DIA. X .050/.051 IN. LONG AFTER TEST
SCALE 9/1

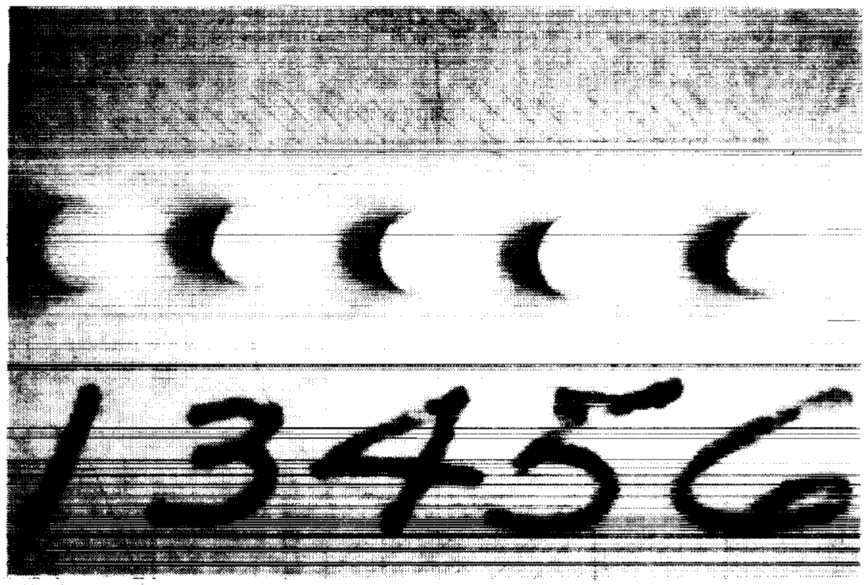

NEG. 7047-1

SIDE I

NEG. 7047-2

OPPOSITE SIDE

Figure 8

COMPRESSION TEST - ZIRCOA "C", .080 ¢ .250 IN. DIA. SPECIMENS

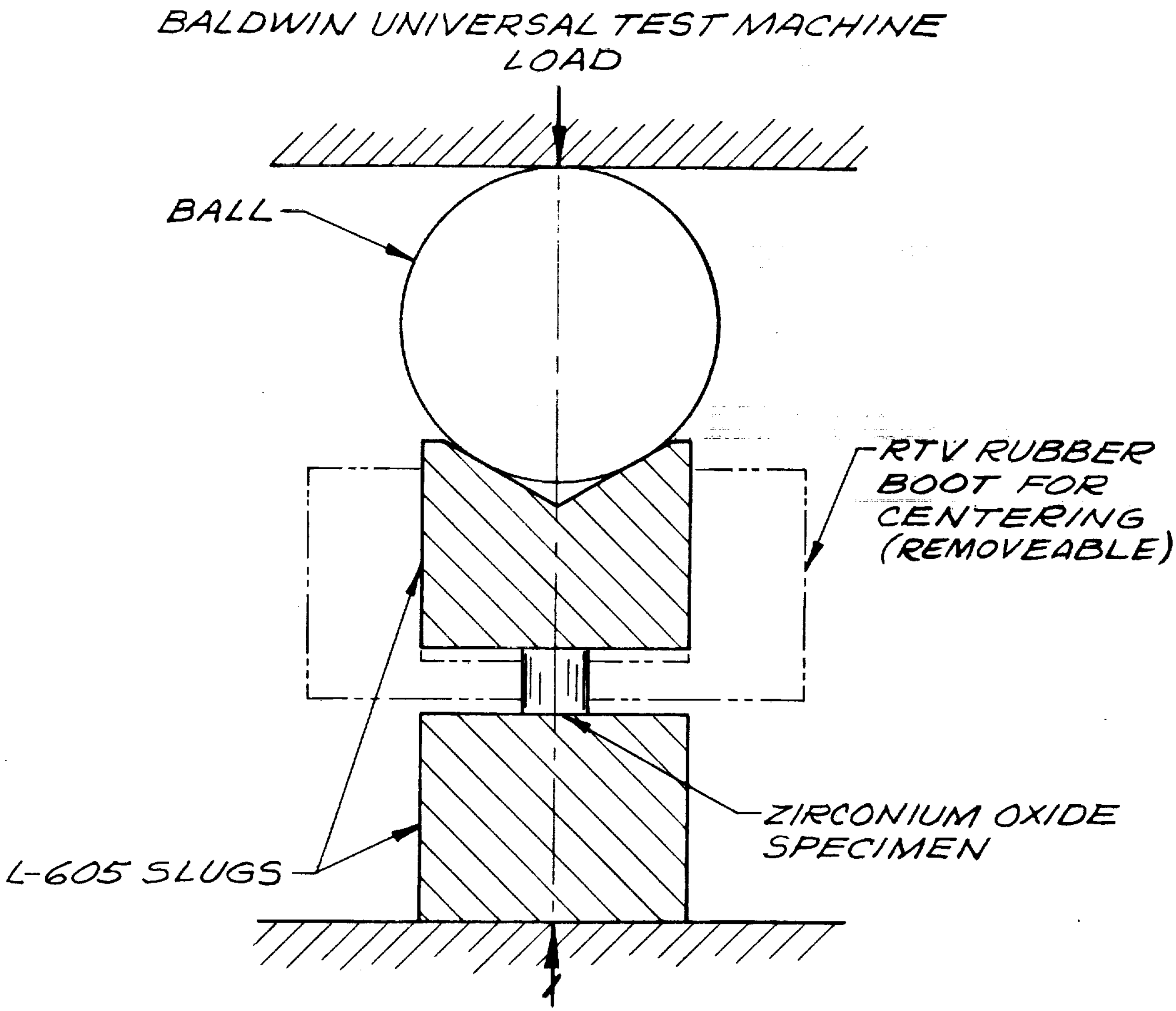

5/1 SCALE

FIGURE 9

TEST RESULTS

ZIRCOA "C", 0.080 IN. DIA. & 0.250 IN. DIA. SPECIMENS

Specimen P/N & Ident.	Applied Load-lbs	Demonstrated Equiv. Compressive Stress - psi x 10^3	Remarks
T-13627 #1	285/290	57	Load applied at 2 lbs/sec, specimen started to powder at 285/290 lbs with simultaneous load rate decrease ($\leq$2 lbs/sec) - stopped loading.
T-13627 #2	165	33	Load applied at 2 lbs/sec, specimen started to powder at 165 lbs.- stopped loading - faces of slugs did not appear to be parallel during loading.
T-13626 #1	4,665	95.2	Load applied at 5 lbs/sec, specimen started to powder at 4,665 lbs load - stopped loading - specimen was removed - one side was crumbled.
T-13626 #2	3,365	68.67	Used 2 layers 0.001 thick silverfoil on each end of specimen. Load applied at 3 lbs/sec, erratic load rate at 1,220 lbs (dropped to 150 lbs). Load increased to 3,000 lbs, cracks appeared slowly - load rate nil - many cracks at 3,300 lbs - stopped load at 3,365 lbs.

FIGURE 10

COMPRESSION TEST OF ZIRCOA "C" CYLINDERS
.080 DIAMETER × .080 HIGH

END NO. 2 SIDE END NO. 1

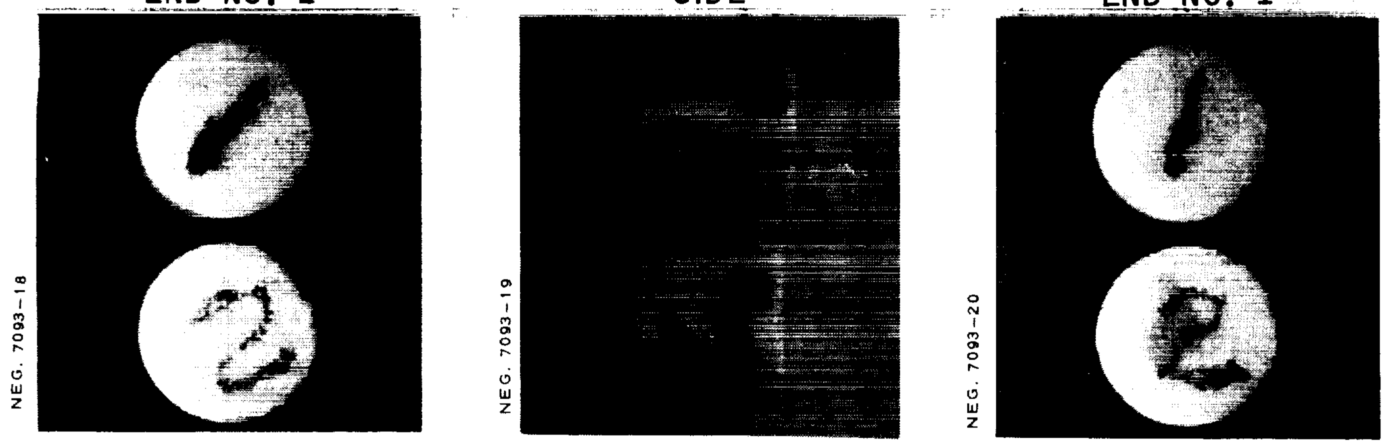

T13627 CYLINDERS, NO'S. 1 & 2, BEFORE TEST
SCALE APPROX. 10/1

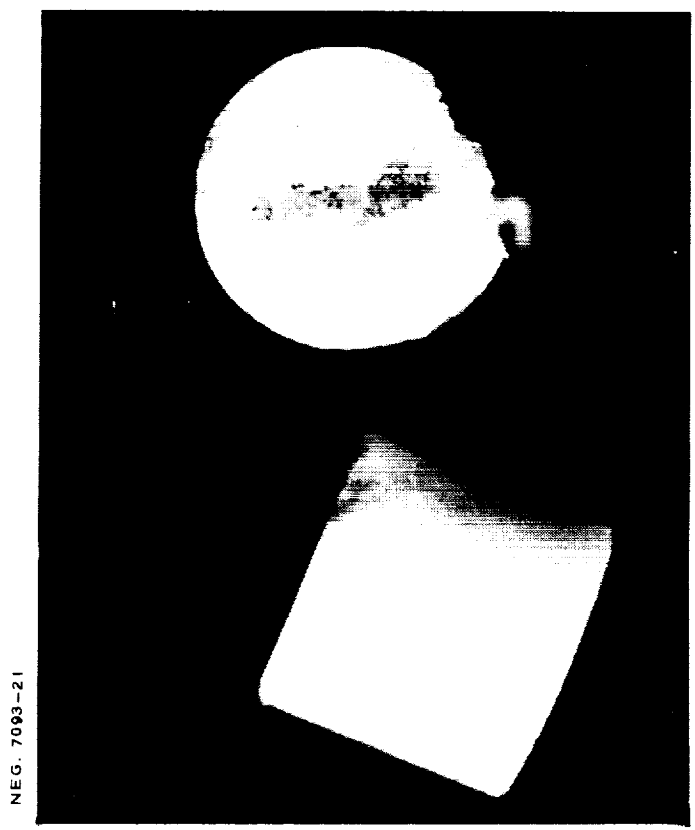

T13627 CYLINDERS, NO'S. 1 & 2, AFTER TEST
SCALE APPROX. 20/1

FIGURE 11

COMPRESSION TEST OF ZIRCOA "C" CYLINDERS
.250 DIAMETER × .250 HIGH

END NO. 2 | SIDE | END NO. 1

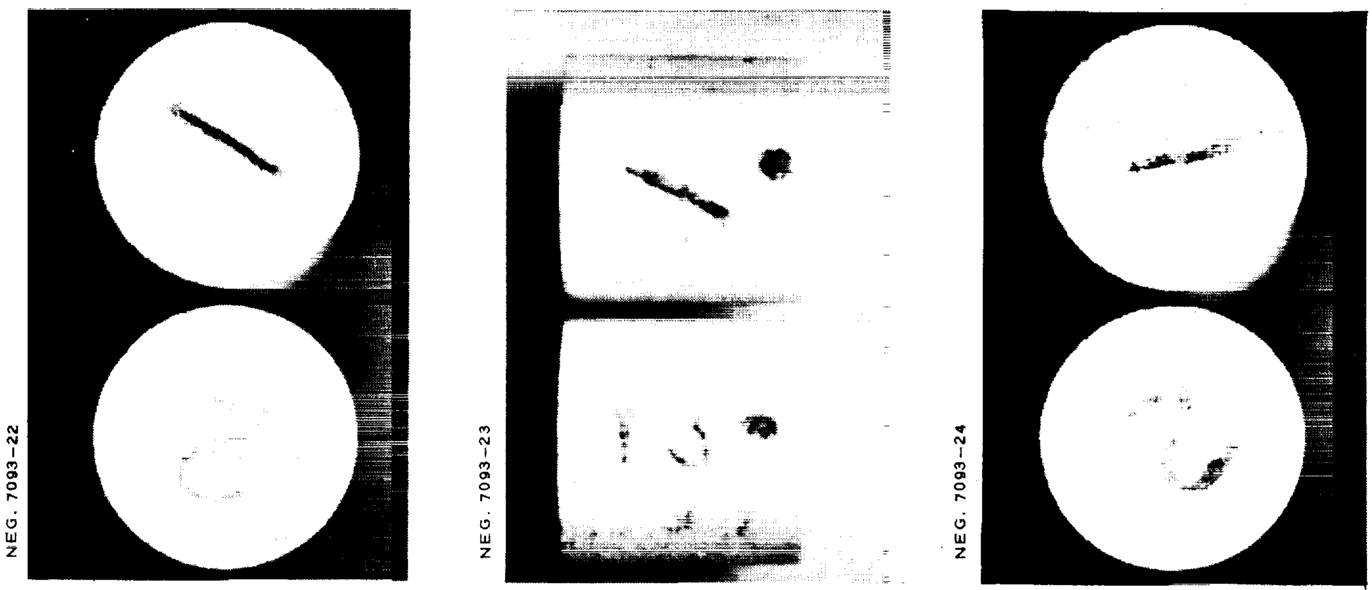

T13626 CYLINDERS, NO'S. 1 & 2, BEFORE TEST
SCALE APPROX. 5/1

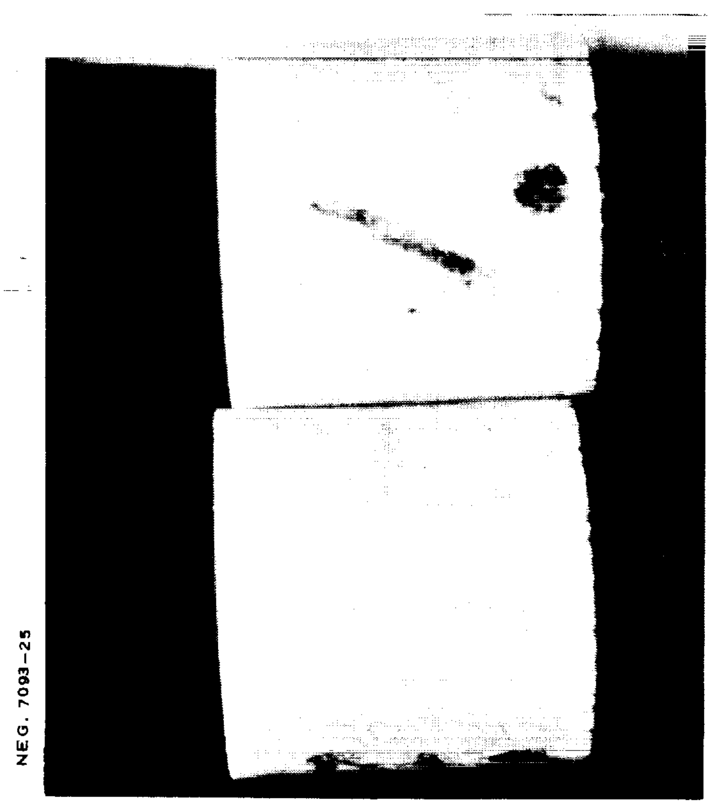

T13626 CYLINDERS, NO'S. 1 & 2, AFTER TEST
SCALE 8/1

FIGURE 12

COMPRESSION TEST- ZIRCOA "C", TRIPLET SPECIMENS

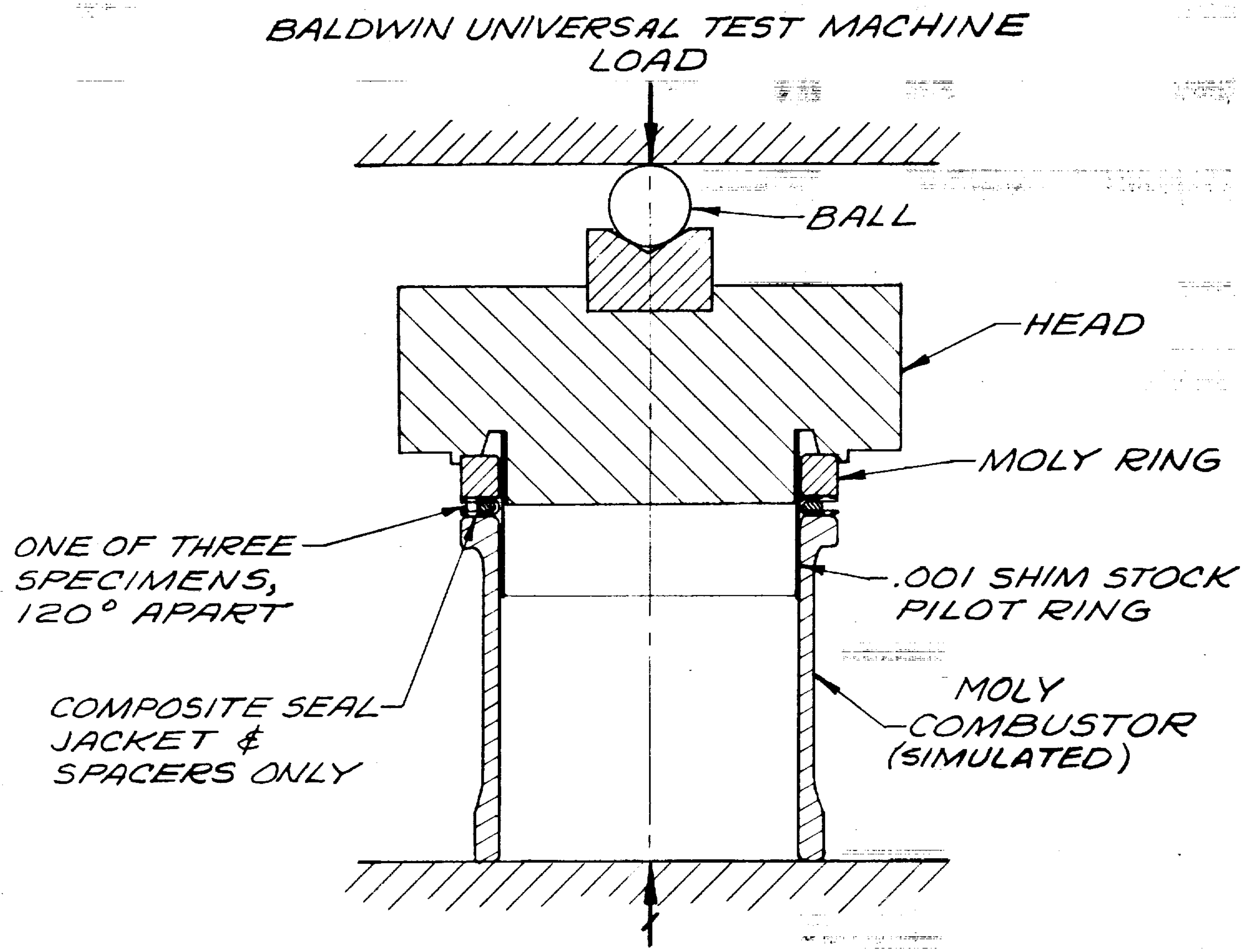

FULL SCALE

FIGURE 13

ZIRCONIUM OXIDE COMPRESSION TEST RESULTS

.053/.054 DIAMETER X .050/.051 IN. LONG TRIPLET SPECIMENS

Material	Triplet Set No.	Applied Load-Lbs. $(\frac{P\ total}{3} = P_{cyl})$	Demonstrated Equiv. Compressive Stress - psi x 10^3	Required Ult. Comp. Strength -psi x 10^3
Zircoa "C" (Full Dense)	1	260*	130	112.95**
	2	296*	148	
	3	270*	135	
Zircoa #1027 (Modified)	1	220*	110	
	2	223*	111.5	
	3	230*	115	
Zircoa "C" (Modified)	1	195*	97.5	
	2	167*	83.5	
	3	175*	87.5	

* Failure load applied at 0.5 - 1 lb/sec.

** Maximum Apollo launch boost limit σ x M.S. (1.5) = Maximum Ult. σ = (75.3 x 1.5) x 10^3 for individual cylinder.

FIGURE 14

COMPRESSION TEST OF T13617 ZIRCOA "C" CYLINDERS
.053 DIAMETER × .050 HIGH

TRIPLET SET NO. 1 BEFORE TEST
SCALE APPROX. 18/1

0° 120° 240°

TRIPLET SET NO. 1 AFTER TEST
SCALE APPROX. 20/1

FIGURE 15

COMPRESSION TEST OF T13617 ZIRCOA "C" CYLINDERS
.053 DIAMETER × .050 HIGH

NEG. 7093-14

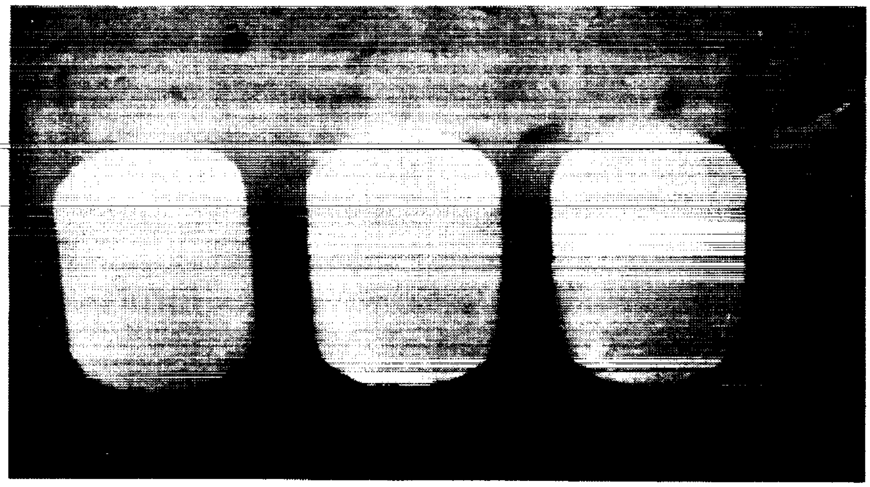

TRIPLET SET NO. 2 BEFORE TEST
SCALE APPROX. 20/1

NEG. 7093-15

6° 126° 246°

TRIPLET SET NO. 2 AFTER TEST
SCALE APPROX. 19/1

FIGURE 16

COMPRESSION TEST OF T13617 ZIRCOA "C" CYLINDERS
.053 DIAMETER × .050 HIGH

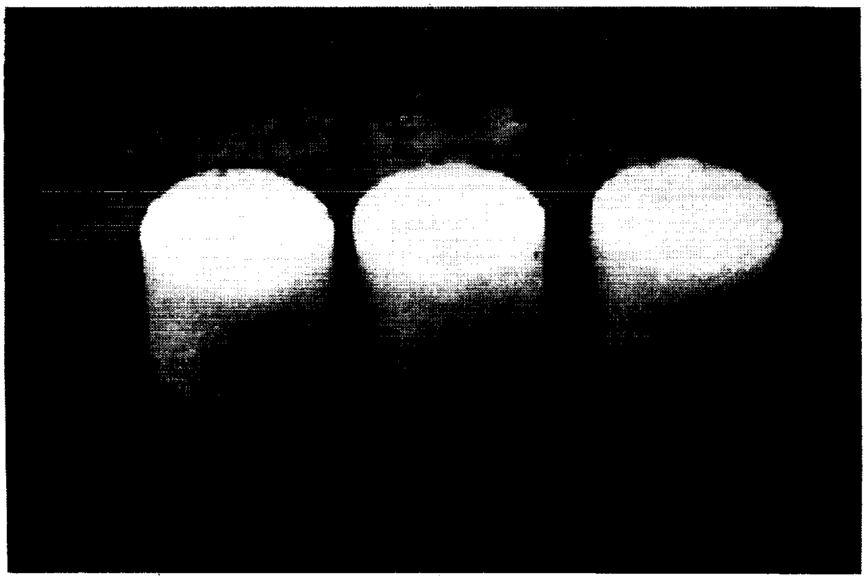

NEG. 7093-16

TRIPLET SET NO. 3 BEFORE TEST
SCALE APPROX. 20/1

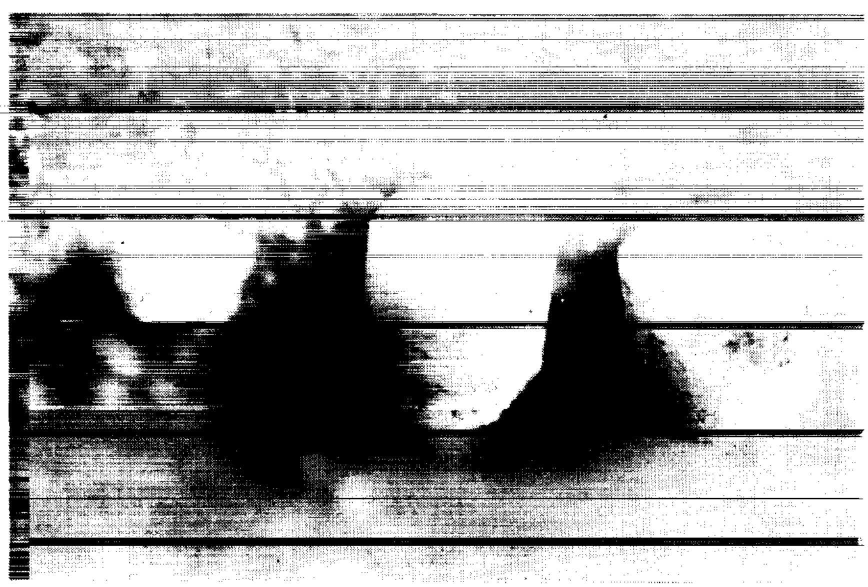

NEG. 7093-17

354° 114° 236°

TRIPLET SET NO. 3 AFTER TEST
SCALE APPROX. 20/1

FIGURE 17

COMPRESSION TEST OF T-13899 CYLINDERS

ZIRCOA "C" (MODIFIED), 0.053 DIAMETER X 0.050 HIGH

TRIPLET SET NO. 1

SCALE APPROX. 17/1

NEG. 8065-1

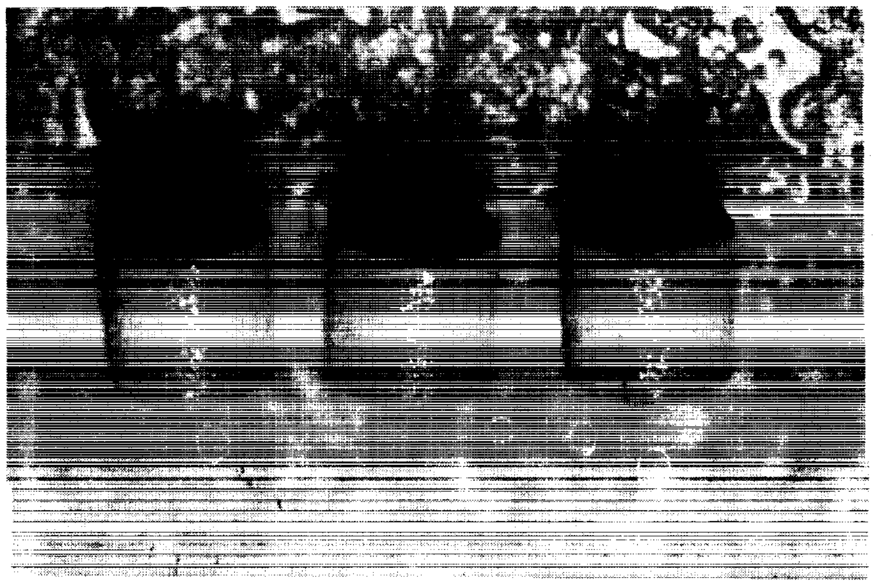

BEFORE TEST

NEG. 8065-2

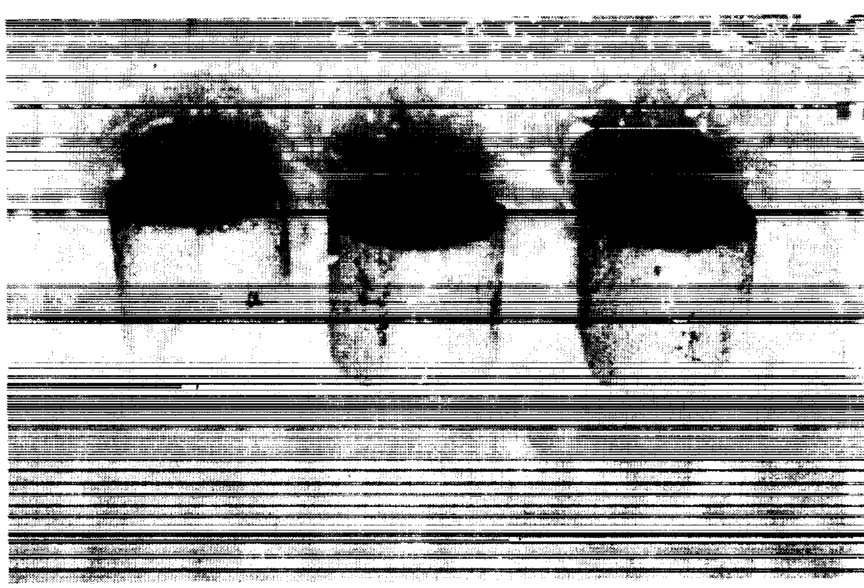

AFTER TEST

FIGURE 18

COMPRESSION TEST OF T-13899 CYLINDERS

ZIRCOA "C" (MODIFIED), 0.053 DIAMETER X 0.050 HIGH

TRIPLET SET NO. 2

SCALE APPROX. 17/1

NEG. 8065-7

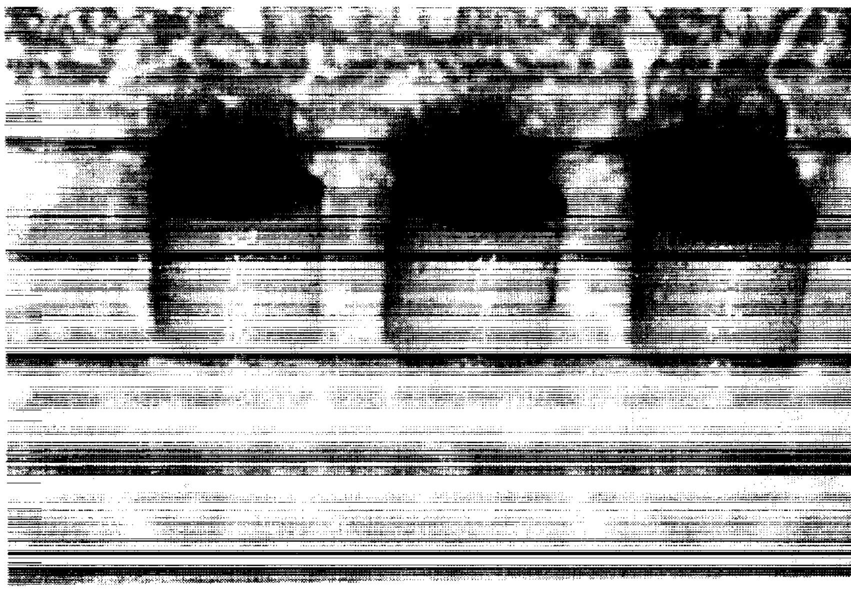

BEFORE TEST

NEG. 8065-8

AFTER TEST

FIGURE 19

COMPRESSION TEST OF T-13899 CYLINDERS

ZIRCOA "C" (MODIFIED), 0.053 DIAMETER X 0.050 HIGH

TRIPLET SET NO. 3
SCALE APPROX. 17/1

NEG. 8065-11

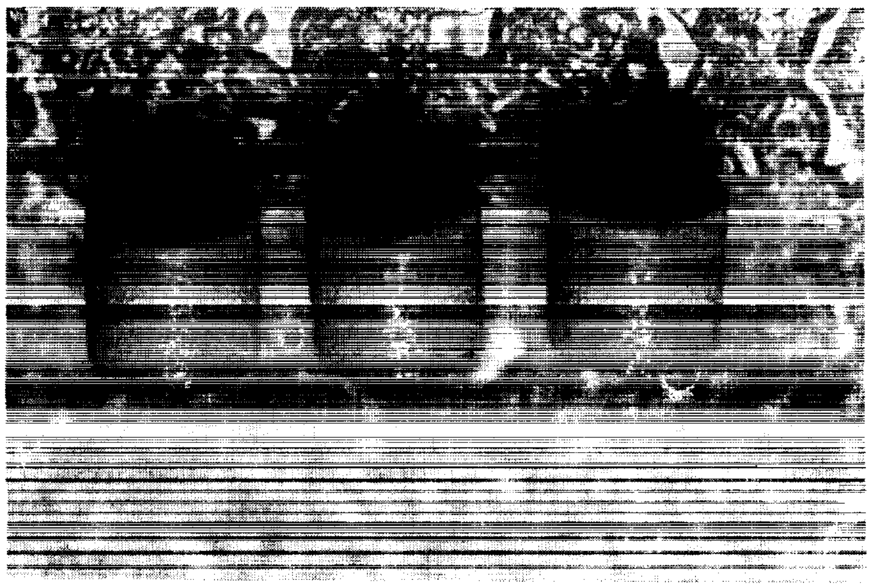

BEFORE TEST

NEG. 8065-12

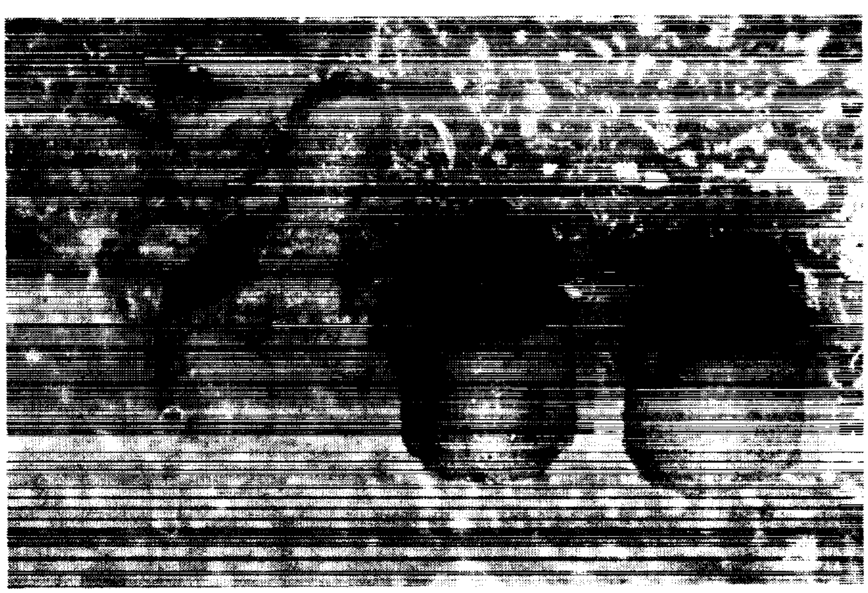

AFTER TEST

FIGURE 20

COMPRESSION TEST OF T-13900 CYLINDERS

ZIRCOA NO. 1027 (MODIFIED), 0.053 DIAMETER X 0.050 HIGH

TRIPLET SET NO. 1
SCALE APPROX. 17/1

NEG. 8065-3

BEFORE TEST

NEG. 8065-4

AFTER TEST

FIGURE 21

COMPRESSION TEST OF T-13900 CYLINDERS

ZIRCOA NO. 1027 (MODIFIED), 0.053 DIAMETER X 0.050 HIGH

TRIPLET SET NO. 2

SCALE APPROX. 17/1

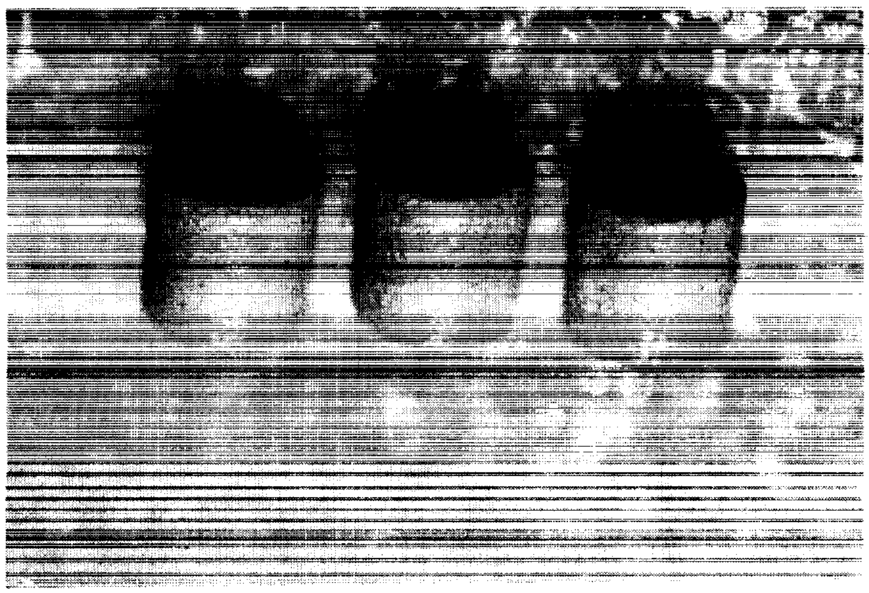

NEG. 8065-5

BEFORE TEST

NEG. 8065-6

AFTER TEST

FIGURE 22

COMPRESSION TEST OF T-13900 CYLINDERS

ZIRCOA NO. 1027 (MODIFIED), 0.053 DIAMETER X 0.050 HIGH

TRIPLET SET NO. 3

SCALE APPROX. 17/1

NEG. 8065-9

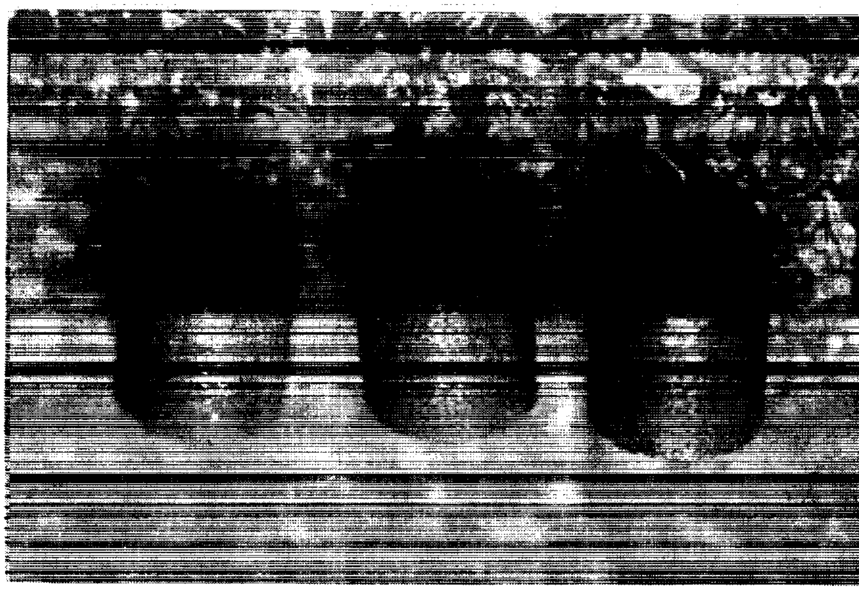

BEFORE TEST

NEG. 8065-10

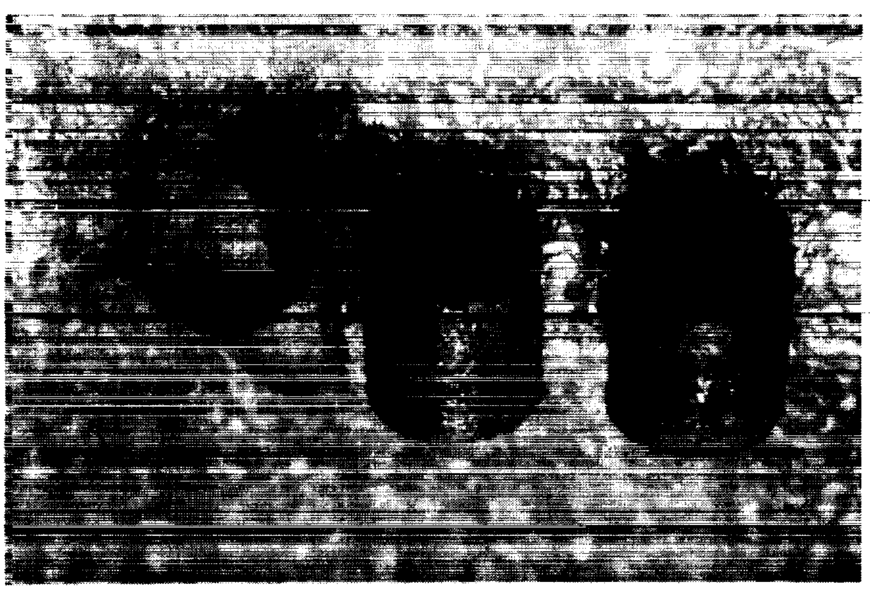

AFTER TEST

FIGURE 23

LOAD TEST-FULL SCALE COMPOSITE SEALS

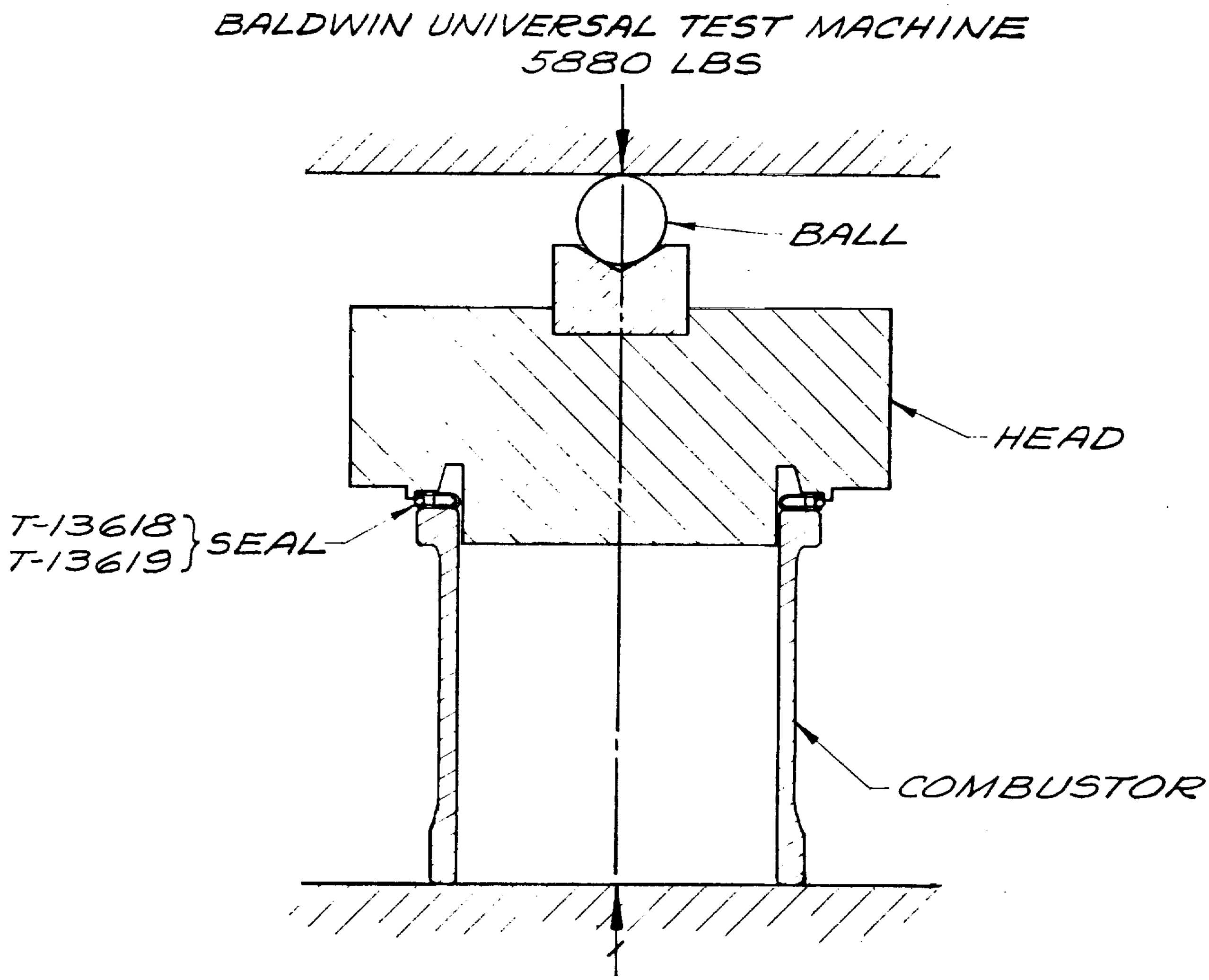

FULL SCALE

FIGURE 24

THE Marquardt CORPORATION VAN NUYS, CALIFORNIA

TEST REPORT

THERMAL RESISTANCE MEASUREMENT OF FULL SCALE SEALS

FOR

APOLLO SERVICE MODULE

REACTION CONTROL SYSTEM ENGINE

CHAMBER SEAL STUDY

PREPARED UNDER CONTRACT NAS 9-4775

TMC 3008

Prepared By C. S. Hill
C. S. Hill
Analysis Engineer

Approved By J. Puntar
J. Puntar
Principal Investigator
Design Engineering

Approved By E P Perlman
E. P. Perlman
Program Manager

CONTENTS

I INTRODUCTION

The thermal resistance of six seal configurations was measured in the Marquardt cold soak facility. The seals tested were made of 6AL-4V Titanium or Rene' 41 and the configurations were as follows:

a. Conical Thinwall
b. Straight Thinwall
c. Composite - With Zirconium Oxide Spacers

II CONCLUSIONS AND RECOMMENDATIONS

Both conical thinwall seals demonstrate thermal resistances higher than 5.0 HR-^{o}F/BTU required to satisfy the program objectives. The composite seals require a design change to obtain a thermal resistance $\geq 5.0 \frac{HR\text{-}^{o}F}{BTU}$. The length/area ratio of the Zirconia cylinders must be approximately doubled. A material with lower thermal conductivity could be substituted if structural criteria could be met.

A problem area associated with high thermal resistance seals was identified. The high thermal expansion coefficient of the aluminum head can cause a thermal short to the chamber at high head temperatures if the chamber is not centered during assembly. The present Apollo assembly procedure does not have a positive center line alignment of the chamber to the injector head. This problem should be eliminated by an assembly procedure change when the high resistance seal is incorporated into the design.

This method of testing has been proven satisfactory for measurement of the thermal resistance of chamber seals. The analytical approach has been verified and can be used for seal design evaluation with a high degree of confidence. The thermal properties of non-standard materials should be verified by test data in future programs during the preliminary design phase before substantial design and development effort has been expended.

III SUMMARY

The composite seal, as designed, does not have a thermal resistance of 5.0 HR-^{o}F/BTU. The actual seal resistance was about 50% lower than theoretical due to a materials property survey error. The measured thermal conductivity of Zirconia was 1.2 BTU/HR-^{o}F-Ft instead of the design value of 0.54 BTU/HR-^{o}F-Ft.

Test results for the thinwall seals showed excellent agreement with theoretical predicted values. The following Table I is a summary of all test results.

TABLE I

SEAL THERMAL RESISTANCE TEST RESULTS

Seal Configuration	P/N	Material	Thermal Resistance			
			Predicted (Neglects Contact Resistance)		Demonstrated	
			Minimum	Maximum	Seal	Joint*
			$\frac{Hr-^oF}{BTU}$	$\frac{Hr-^oF}{BTU}$	$\frac{Hr-^oF}{BTU}$	$\frac{Hr-^oF}{BTU}$
Conical Thinwall	T-13622	Titanium	5.3	6.2	6.6	5.7
	T-13621	Rene' 41	3.7	4.3	5.2	4.6
Straight Thinwall	T-13611	Titanium	1.8	2.2	2.1	2.0
	T-13612	Rene' 41	1.2	1.5	1.3	1.2
Composite	T-13618	Titanium	4.7	5.3	3.0	2.8
	T-13619	Rene' 41	3.8	4.3	2.8	2.6
Zirconia Cylinder	T-13617	Zirconia	8.1	8.3	3.5	3.2

*Overall thermal resistance of head/seal/chamber

IV TEST PROCEDURE

Each seal was assembled into the thermal test rig and tested in the cold soak test facility. Figure 1 is a photograph of assembled test hardware. A chronological test history is shown in Appendix A, Figure 2. The seal configurations tested are shown in Figure 3. Figure 4 is a detail summary of the measured thermal resistances. A photograph of the facility is shown in Figure 5, Appendix A.

Thermal resistance was measured using the general procedures outlined in MTP 0041, Appendix B which contains a schematic of the test setup, the instrumentation, and the detailed test procedure used.

A modification of the test procedure was made because the large heat capacity of the thermal radiator and the low rate of radiation heat transfer required excessive test time to reach complete thermal equilibrium. The low heat capacity of the simulated injector head allowed the test head to reach steady state temperatures at a constant heat input while the radiator did not change temperature significantly. Therefore, measurements were made prior to reaching complete thermal equilibrium of the radiator. Several measurements of the heat flow and the resulting temperature difference were taken and used to calculate the joint thermal resistance.

A typical time-temperature history of a test item during a data period is shown below:

TEST ITEM - TIME HISTORY

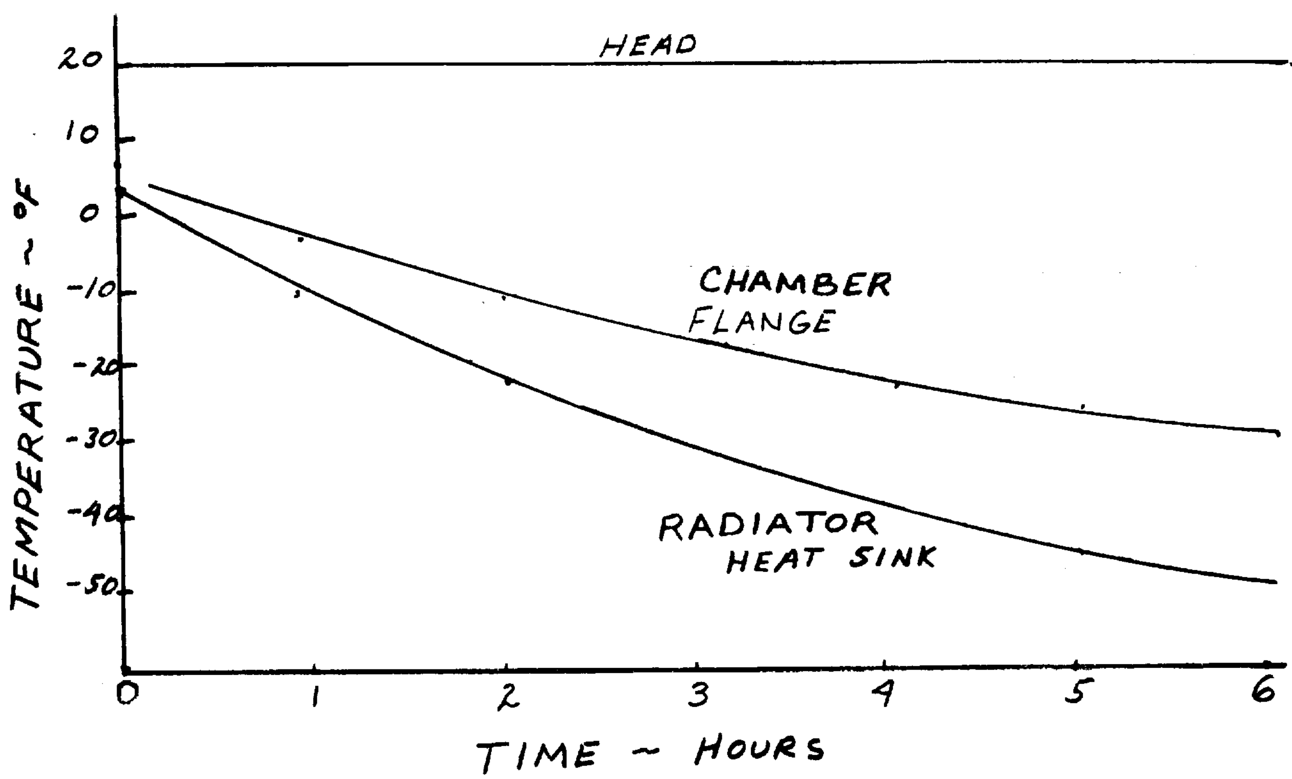

V SEAL RESISTANCE CALCULATION PROCEDURE

The heat paths across the head-seal-chamber joint are shown below:

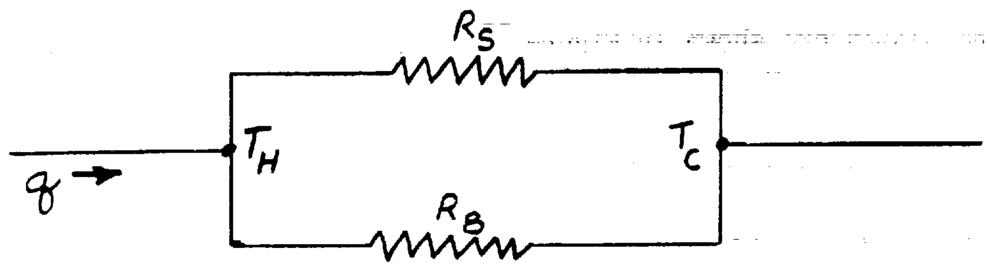

where:

R_J = Total Joint Thermal Resistance

R_B = Attach Hardware Thermal Resistance $\frac{HR\text{-}^{\circ}F}{BTU}$

R_S = Seal Thermal Resistance $\frac{HR\text{-}^{\circ}F}{BTU}$

T_H = Temperature of Simulated Head

T_C = Chamber Flange Temperature

q = Heat Flow Rate - $\frac{BTU}{HR}$

The joint overall thermal resistance (R_J) was calculated by dividing the temperature difference ($T_H - T_C$) between the injector head and the chamber flange by the heat flow rate (q), $R_J = \frac{T_H - T_C}{q} \quad \frac{^{\circ}F}{(BTU/Hr)}$. The joint resistance is equal to

$$R_{joint} = \frac{R_S \; R_B}{R_S + R_B}$$

and therefore

$$R_S = \frac{R_B \; R_J}{(R_B - R_J)}$$

Seal resistance was calculated from $R = \frac{R_B \; R_J}{(R_B - R_J)}$ where bolt thermal resistance (R_B) was calculated to be 42.3 $\frac{HR-{}^\circ F}{BTU}$ from the nominal dimensions of the attach hardware. Heat losses by convection were negligible at high vacuum, $< 10^{-5}$ mm Hg. Radiation heat losses from the simulated injector to the guard boundary were made $\approx$ zero by heating the boundary to the same temperature as the simulated injector head.

Several heat flow rates were measured and the joint thermal resistance averaged to calculate the seal thermal resistance. Appendix B contains a summary of the data used to calculate joint resistance for seal resistance tests 1 through 4.

VI DISCUSSION OF TEST RESULTS

Thermal resistance testing of the thinwall seals was very successful. Measured results were close to the predicted thermal resistances. Test thermal resistance values were repeatable within 15% from high temperature to low temperature and within 10% or less during the run.

Conical seal thermal resistances were slightly higher than the predicted maximum indicating the analysis to be conservative. This agreement is excellent considering contact resistance was neglected in the analysis and conservative simplifying assumptions were made with the complicated shaped areas.

Thermal shorting between injector head and chamber occurred during high temperature testing of titanium straight thinwall seal. Additional tests were made to verify the temperature dependency of the thermal short. Cause of the short was determined to be off center assembly of the chamber to the test item. The high thermal expansion coefficient of the aluminum head caused the register diameter of the injector to contact the chamber inside diameter. This lowered the joint thermal resistance to 0.75 $\frac{HR-{}^\circ F}{BTU}$.

Present Apollo assembly procedures have no centering requirement of chamber with injector. A change in engine chamber-injector assembly procedure will be required when any high resistance seal is incorporated into the engine.

COMPOSITE SEAL

The thermal resistances of the composite seals were about 50% less than the calculated minimum. Analysis indicated the most probable cause to be low thermal resistance through the Zirconia cylinders. An additional test (#4), was run to verify this conclusion. Only the Zirconia cylinders from the Titanium composite seal were assembled into the test item to isolate that heat path. The measured thermal resistance was 3.5 HR-^{o}F/BTU.

The theoretical resistance of the cylinders is 8.0 HR-^{o}F/BTU. Dimensions of the cylinders were identical to those used in the analysis, therefore, thermal conductivity of the Zirconia was $\approx$ 1.2 BTU/HR-^{o}F-Ft rather than 0.54 BTU/HR-^{o}F-Ft which was used as design criteria.

The composite seal design requires a Zirconia segment thermal resistance of $\geq$ 8.0 HR-^{o}F/BTU to achieve an overall minimum resistance of $\geq$ 5.0 HR-^{o}F/BTU. Therefore, the ratio of length to heat transfer area of the Zirconia cylinders must be $\approx$ doubled or a lower conductivity material substituted to satisfy the program objectives.

APPENDIX A

CONTENTS


TEST 11267 SEAL THERMAL RESISTANCE TEST HARDWARE
BLDG. 32
11 JAN 66 (u)

FIGURE 1

The following table summarizes the thermal testing:

FIGURE 2

TEST HISTORY

THERMAL RESISTANCE TEST #	RUN #	HEAD TEMPERATURE °F	PURPOSE
Test #1 - Dec. 18-21, 1965			
Titanium Seals	1	20	Measure thermal resistance (R_S) @ 0°F
Item 1 - T-13622	2	130	Increase heat flow across seal for greater accuracy
Item 2 - T-13611	3	20	Verify Run 1
	4	130	Verify Run 2
	5	60	Verify thermal short dependency on assembly temperature
Test #2 - Dec. 30, 1965			
Rene' 41 Conical T-13621	1	20	Measure R_S at 0°F
Rene' 41 Thinwall T-13612	2	160	Increase heat flow across seal for greater accuracy
Test #3 - Jan. 13-14, 1966			
Composite Seals	1	20	Measure R_S at 0°F
Titanium T-13618 Rene' 41 T-13619	2	160	Increase heat flow across seal for greater accuracy
Test #4 - Jan. 21, 1966			
Unplanned test to define problem with composite seal low resistance	1	20	Measure thermal conductivity of the Zirconia cylinders and effect of bumper segments
	2	160	

SPECIMEN DESCRIPTION - FULL SCALE SEALS						
COMPOSITE (0.090/0.095 LONG)		STRAIGHT THINWALL (0.090/0.095 LONG)		CONICAL THINWALL (0.248/0.252 LONG)		TYPE
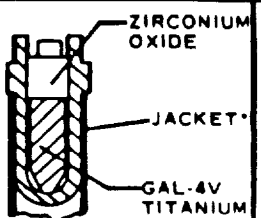 ZIRCONIUM OXIDE; JACKET*; 6AL-4V TITANIUM				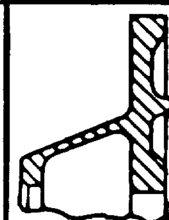		CROSS SECTION OF SEAL
T-13618	T-13619	T-13611	T-13612	T-13622	T-13621	PART NUMBER
*6AL-4V TITANIUM	*RENE' 41	6AL-4V TITANIUM	RENE' 41	6AL-4V TITANIUM	RENE' 41	MATERIALS
4.87/5.26	3.77/4.30	1.82/2.21	1.21/1.48	5.30/6.20	3.68/4.33	THERMAL RESISTANCE ⚠1

⚠1 Predicted thermal resistance
$= \frac{HR-{}^{o}F}{BTU}$
Neglects contact resistance

PREPARED BY C. S. HILL

CHECKED BY

CLASSIFICATION

THE MARQUARDT CORPORATION

PAGE

REPORT

DATE FEB 6, 1966

SEAL THERMAL RESISTANCE TEST RESULTS

DESIGN CONFIGURATION	PART NUMBER	MAT'L	THERMAL RESISTANCE HR - °F/BTU: TEST JOINT 20 °F	TEST JOINT 150 °F	TEST SEAL 20 °F	TEST SEAL 150 °F	PREDICTED MINIMUM SEAL
CONICAL THINWALL	T-13622	6AL-4V	6.0	5.7	7.0	6.6	5.30
	T-13621	RENE'41	4.8	4.6	5.4	5.2	3.68
STRAIGHT THINWALL	T-13611	6AL-4V	2.0	.75	2.1	—	1.82
	T-13612	RENE'41	1.4	1.2	1.5	1.3	1.21
COMPOSITE SEAL ASSEMBLY	T-13618	6-AL-4V ZIRCONIA	2.7	2.8	2.9	3.0	4.67
	T-13619	RENE'41 ZIRCONIA	2.2	2.6	2.3	2.8	3.77
ZIRCONIA CYLINDERS	T-13617	ZIRCONIA	3.8*	3.2	4.2*	3.5	8.08
COMPOSITE WITHOUT SEGMENT SET-OR SNAP RING	T-13613 T-13617	RENE'41 ZIRCONIA	3.2*	2.3	3.6*	2.5	3.77

* NOT ACCURATE DUE TO SMALL TEMPERATURE DIFFERENCE

FIGURE 4

FIGURE 4

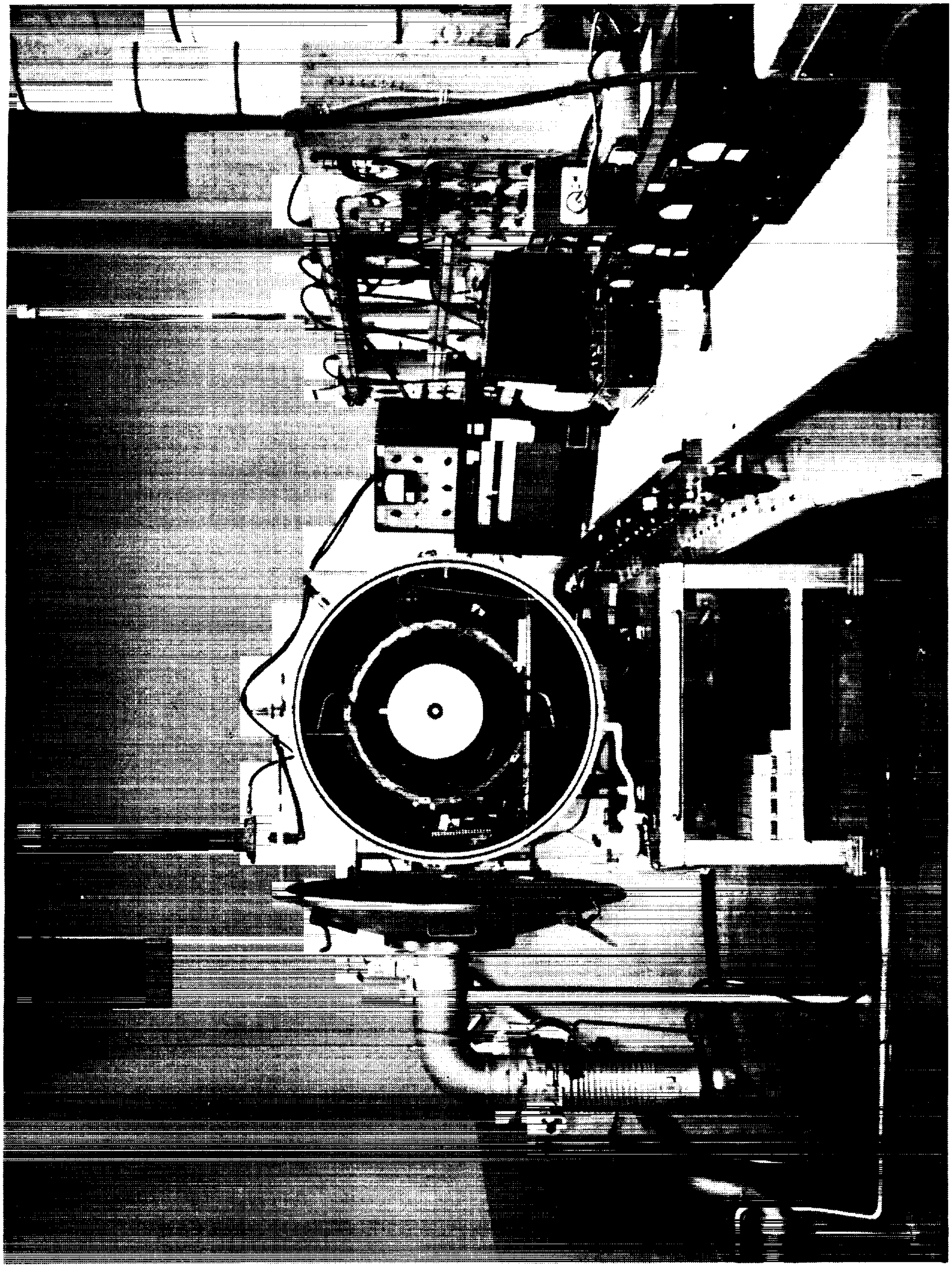

TEST 11267 3008 SEAL THERMAL RESISTANCE TEST SETUP
BLDG. 32 (U)
21 DEC 65

NEG. T11267-2

FIGURE 5

APPENDIX B

TEST DATA SUMMARY SHEETS

SEAL TEST # 1 DATE DEC 18-21 1965

	CONICAL TITANIUM							THINWALL TITANIUM						
RUN / DATA POINT	T_{HEAD} °F	T_{FLANGE} °F	ΔT °F	HEAT BTU/HR	JOINT R_{TM} HR-°F/BTU	SEAL R_{TH}	SEAL TEMP °F	T_H °F	T_F °F	ΔT °F	Q BTU/HR	R_J HR-°F/BTU	R_S HR-°F/BTU	T_S °F
1 / [illegible]	+20	-29	49	8.54	5.73	6.63	-4.5	+20	-7	27	12.53	2.16	2.28	6.5
1 / [illegible]	+20	-30	50	8.59	5.82	6.75	-5.0	+20	-8	28	13.88	2.[illegible]	2.12	6.[illegible]
1 / 1250	+20	-30	50	7.95	6.29	7.39	-5.0	+20	-8	28	13.00	2.1[illegible]	2.27	6.0
1 / [illegible]	+20	-34	54	8.58	6.2[illegible]	7.39	-7.	+20	-10	30	13.60	2.21	2.3[illegible]	5.0
2 / 0240	+131	+17	114	19.78	5.16	6.81	74.0	131	100	31	41.56	0.75	0.75	115.5
2 / [illegible]	130	17	113	19.78	5.71	6.[illegible]	73.5	131	100	31	41.56	0.75	0.75	11[illegible]
2 / 0340	130	17	113	20.11	5.62	6.48	73.5	131	100	31	41.56	0.75	0.25	115.5
3 / 1230	+20	-47	67	10.7	6.24	7.34	-13.	+20	-15	35	16.4	2.13	2.24	2.5
3 / 1300	+20	-48	68	10.9	6.24	7.3[illegible]	-14.0	+20	-15	35	16.8	2.08	2.19	2.5
3 / 1315	+20	-48	68	11.3	6.02	7.[illegible]	-14.0	+20	-15	35	16.8	2.08	2.1[illegible]	2.5
4 / 1734	129	+7	122	23.0	5.30	6.[illegible]	64.[illegible]	129	+25	34	47.2	0.72	0.73	112.0
5 / 2115	60	-15	75	12.47	6.01	[illegible]	22.5	61	20	41	22.[illegible]	1.81	1.[illegible]	40.5
5 / 2145	60	-15	75	12.66	5.92	6.88	22.5	60	20	40	20.13	1.79	2.[illegible]	40.0
5 / 2200	60	-15	75	12.66	5.92	6.88	22.5	60	20	40	20.21	1.80	1.33	40.0
5 / 2245	60	-16	75	12.64	5.92	6.84	[illegible]	59	19	40	20.21	1.80	1.88	39.0

SEAL TEST # 2 DATE DEC 30, 1965

	CONICAL RENE							THINWALL RENE						
RUN / DATA POINT	T_H °F	T_F °F	ΔT °F	Q BTU/HR	R_J HR-°F/BTU	R_S HR-°F/BTU	T_S °F	T_H °F	T_F °F	ΔT °F	Q BTU/HR	R_J HR-°F/BTU	R_S HR-°F/BTU	T_S °F
1 / 1515	20.5	-34	54.5	11.5	4.74	5.34	-6.75	20	-6	26	17.6	1.48	1.53	7.0
1 / 1520	20	-38	58	11.5	5.04	5.72	-1	18	-8	26	17.5	1.49	1.54	5.[illegible]
1 / 1530	20	-40	60	12.5	4.80	5.41	-1[illegible]	19	-8	27	20.2	1.34	1.38	[illegible]
1 / 1540	20.5	-40	60.5	12.5	4.84	5.47	-1[illegible]	20	-8	28	19.3	1.45	1.50	[illegible]
				AVER	4.86					AVER		1.44		
2 / 1750	160	18	142	32.3	4.40	4.91	[illegible]	160	90	70	58.8	1.19	1.22	12[illegible]
2 / 1810	160	20	140	30.2	4.64	5.21	70.0	160	92	68	56.0	1.21	1.25	126.0
2 / 1820	161	22	139	28.2	4.93	5.58	71.5	161	93	68	53.8	1.26	1.30	127.0
2 / 1830	160	22	138	29.7	4.65	5.22	71.0	161	95	66	53.8	1.23	1.27	129
2 / 1845	160	23	137	29.7	4.61	5.17	71.[illegible]	162	96	66	53.4	1.24	1.27	1.29
				AVER	4.65						AVER	1.23		

PREPARED BY
CHECKED BY
CLASSIFICATION

THE MARQUARDT CORPORATION

PAGE
REPORT
DATE

SEAL TEST # 3 DATE JAN 13-14, 1966

	COMPOSITE - TITANIUM							COMPOSITE - RENE						
RUN / DATA POINT	T_H °F	T_F °F	ΔT °F	Q BTU/HR	R_J HR-°F/BTU	R_S HR-°F/BTU	T_S °F	T_N °F	T_F °F	ΔT °F	Q BTU/HR	R_J HR-°F/BTU	R_S HR-°F/BTU	T_S °F
1 / 1410	159	69	90	31.6	2.85	3.06	114.0	157	80	77	35.8	2.15	2.27	118.5
1 / 1425	160	69	91	35.2	2.54	2.76	114.5	161	82	79	[illegible]	2.15	2.27	[illegible]
1 / 1445	162	70	92	34.0	2.71	2.90	116.	162	82	80	[illegible]	2.31	2.44	[illegible]
1 / 1500	161	71	90	32.8	2.74	2.93	[illegible]	161	82	79	[illegible]	2.28	2.41	122.0
1 / 1520	160	70	90	32.8	2.74	2.93	115.0	160	82	78	34.6	2.25	2.38	121.0
			Aver.		2.73						Aver.	2.23		
2 / 1338	21	-19	40	13.7	2.92	3.14	1.0	21	-10	31	11.8	2.63	2.80	5.5
2 / 1352	20	-19	39	13.7	2.85	3.06	.5	19	-11	30	11.8	2.54	2.70	4.0
2 / 1423	19	-20	39	13.8	2.83	3.03	-.5	20	-11	31	12.1	2.56	2.73	4.5
2 / 1435	19	-21	40	13.8	2.90	3.11	-1.0	20	-12	32	12.3	2.60	2.77	4.0
2 / 1500	21	-21	42	16.1	2.61	2.72	0	21	-12	33	13.9	2.37	2.51	4.5
			Aver.		2.82						Aver.	2.54		

TMC A605

PREPARED BY ______
CHECKED BY ______
CLASSIFICATION ______

THE MARQUARDT CORPORATION

PAGE ______
REPORT ______
DATE ______

SEAL TEST # 4 DATE JAN 21, 1966

ZIRCONIA - ONLY | NO BUMPERS - RENE

RUN / DATA POINT	T_H °F	T_F °F	ΔT °F	Q BTU/HR	R_J HR-°F/BTU	R_S HR-°F/BTU	T_S °F	T_H °F	T_F °F	ΔT °F	Q BTU/HR	R_J HR-°F/BTU	R_S HR-°F/BTU	T_S °F
1 / 1300	19.5	0	19.5	5.32	3.67	4.01	9.75	18	8	10	3.58	2.79	2.99	13.0
2 / 1315	19.[illegible]	-1	20	5.[illegible]	3.77	4.14	9.0	18	7	11	3.67	3.00	3.23	[illegible]
3 / 1330	18	-3	21	5.[illegible]	3.[illegible]	4.36	7.5	17	5	12	3.[illegible]	3.[illegible]	3.57	11.[illegible]
4 / 1345	17	-4	21	5.52	3.95	4.36	6.5	16	4	12	3.[illegible]	3.32	3.63	11.0
				AVE	3.84						AVG.	3.20		
1 / 1430	153	42	111	35.8	3.10	3.35	97.5	154	63	91	42.7	2.13	2.24	108.5
2 / 1545	167	52	115	35.[illegible]	3.24	3.51	10[illegible]	169	75	94	40.3	2.33	2.47	84.5
2 / 1600	169	53	116	35.6	3.26	3.53	111.0	170	76	94	40.3	2.33	2.47	123.0
				AVERAGE	3.20						AVER.	2.26		

THE Marquardt CORPORATION VAN NUYS, CALIFORNIA

TEST REPORT

SUPPLEMENTAL THERMAL EVALUATION

OF

EXPERIMENTAL ZIRCONIUM OXIDE MATERIALS

FOR

APOLLO SERVICE MODULE

REACTION CONTROL SYSTEM ENGINE

CHAMBER SEAL STUDY

PREPARED UNDER CONTRACT NAS 9-4775

TMC 3008

Prepared by J C Paladin
J. C. Paladin
Development Engineer

Approved by J Puntar
J. Puntar
Principal Investigator
Design Engineering

Approved by E. P. Perlman
E. Perlman
Program Manager

TABLE OF CONTENTS

LIST OF ILLUSTRATIONS

I. INTRODUCTION

Initial full scale seal thermal resistance tests of composite seals with full density Zircoa "C" cylinder spacers indicated that seal resistance was about 3.0 Hr-°F/Btu and not the expected 5.0 Hr-°F/Btu. Subsequent tests were conducted to measure thermal conductivity of the full density Zircoa "C" (347 lb/ ft^3). It was discovered that the conductivity was 1.2 Btu/Hr-Ft°F rather than the assumed 0.54 Btu/Hr-Ft°F.

A literature survey was made and it was found that thermal conductivity of zirconium oxide could be controlled by varying it's bulk density. (Figure 15a of Reference 1)

The supplier of the Zircoa "C" was contacted and he verified that porosity (and thus density) of Zircoa "C" could be controlled. By the information shown on the above referenced Figure, it appeared that modified Zircoa "C" with bulk density of 270 lbs/ft^3 might have a thermal conductivity approaching the required 0.54 Btu/Hr-Ft°F. The compressive strength, however, of modified Zircoa "C" was anticipated to be marginal. The vendor suggested that another grade of zirconium oxide, Zircoa 1027, which possesses compressive strength approximately 30% greater than Zircoa "C", also be evaluated at the same bulk density.

A set of 60 cylinders of each of the above, modified Zircoa "C" and modified Zircoa 1027, were manufactured and tested for thermal conductivity in accordance with the test method previously employed in evaluating the full dense Zircoa "C".

II. CONCLUSIONS AND RECOMMENDATIONS

Neither of the two types of experimental Zirconium Oxide tested, Zircoa No. 1027 (Modified) or Zircoa "C" (Modified), exhibited sufficiently high thermal resistance to meet the program objective.

Minimum acceptable resistance of the heat path through the cylinders is 8.0 Hr-°F/Btu. The Zircoa "C" (Modified) had an average resistance of 5.0 Hr-°F/Btu and Zircoa 1027 (Modified) had an average resistance of 3.5 Hr-°F/Btu.

The relationship of porosity (bulk density) of Zircoa "C" and its thermal conductivity is not as reported in Figure 15a of Reference 1. Based on results of this test, a higher degree of porosity of the Zirconium Oxide is required for the necessary high thermal resistance. For this high porosity, the compressive strength of the cylinders would be less than adequate.

It is recommended that the alternate methods of obtaining high resistance of the composite seal be reconsidered. The most feasible method would be to double the ratio of the existing Zirconium Oxide cylinder length to heat transfer area.

III. SUMMARY

One set of cylinders from each of the two types of experimental Zirconium Oxide which were selected for further study were tested for their thermal resistance in test rigs which were made to simulate Apollo SM/RCS engines.

Testing was performed in Marquardt's high altitude, cold wall, space simulator chamber. The materials which were tested and the measured thermal resistances of 60 cylinders (required quantity per composite seal) are shown below:

Material	Bulk Density lbs/ft^3	Thermal Resistance Hr-°F/Btu
Zircoa "C" (Modified	269	5.0
Zircoa 1027 (Modified)	275	3.5

IV. TEST HARDWARE

Both sets of Zirconium Oxide cylinders were assembled into simulated Apollo SM/RCS engines consisting of flight-type Apollo combustion chambers, attach rings and bolts and machined aluminum blocks to simulate engine injector heads. A detail of cylinder assemblies is shown in Figure 1. The composite seal jacket, which provides the second heat path in the composite seal, was not used in order to facilitate direct measurement of the cylinder heat path resistance only.

The two simulated engines were then suspended from a bar, with the simulated engine injector heads encased in an aluminum thermal boundary. A photograph of a similar test rig prior to installation into the cold wall vacuum chamber is shown in Figure 2.

Figure 3 schematically shows the locations of engine and facility thermocouples.

V. TEST PROCEDURE

Testing was conducted per Appendix B of MTP 0041. Throughout testing, the facility chamber pressure was maintained at 9×10^{-6} mm Hg or less. Chamber walls were cooled by liquid nitrogen to about -320°F. Simulated engine injector heads and the thermal boundary were then heated to the same desired run temperature to prevent radiation heat loss from the simulated injector heads. Run temperatures were maintained constant for one hour during which time data were recorded.

Two record runs were made during this test. One was at a nominal simulated injector head temperature of +20°F (cylinder temperature ≅ 0°F) and one at +160°F.

VI. SEAL RESISTANCE CALCULATION PROCEDURE

The heat paths across the head-seal-chamber joint are shown below:

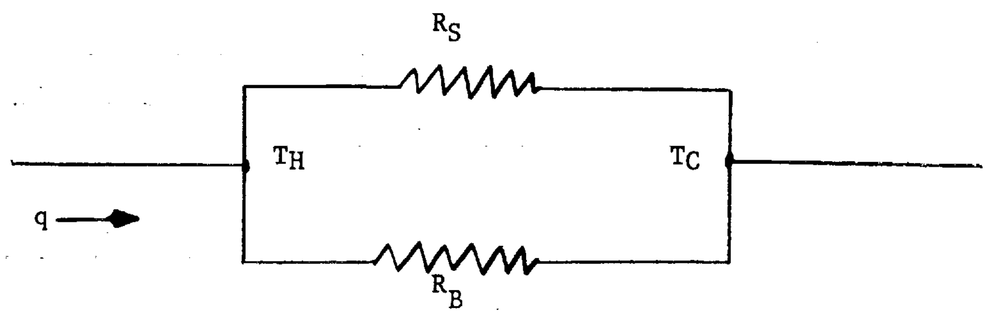

where:

R_J = Total Joint Thermal Resistance

R_B = Attach Hardware Thermal Resistance $\frac{Hr-°F}{BTU}$

R_S = Seal Thermal Resistance $\frac{Hr-°F}{BTU}$

T_H = Temperature of Simulated Head

T_C = Chamber Flange Temperature

q = Heat Flow Rate - $\frac{BTU}{Hr.}$

The joint overall thermal resistance (R_J) was calculated by dividing the temperature difference (T_H - T_C) between the injector head and the chamber flange by the heat flow rate (q),

$$R_J = \frac{T_H - T_C}{q} \quad \frac{°F}{(BTU/Hr)} .$$

The joint resistance is equal to

$$R_{joint} = \frac{R_S \quad R_B}{R_S + R_B}$$

and therefore

$$R_S = \frac{R_B \quad R_J}{(R_B - R_J)}$$

Seal resistance was calculated from $R = \frac{R_B \quad R_J}{(R_B - R_J)}$ where bolt thermal resistance (R_B) was calculated to be 42.3 Hr-°F/BTU from the nominal dimensions of the attach hardware. Heat losses by convection were negligible at high vacuum, $< 10^{-5}$ mm Hg. Radiation heat losses from the simulated injector heads to the thermal boundary were made approximately zero by heating the thermal boundary to the same temperature as the simulated injector heads.

VII. DISCUSSION OF TEST RESULTS

Thermal resistances which were obtained for the two types of Zirconium Oxide cylinders tested are:

Material	Thermal Resistance Hr-°F/BTU
Zircoa "C" (Modified)	5.0
Zircoa 1027 (Modified)	3.5

Both of the above resistances are average values calculated from results of two separate heat flow rates (engine simulated injector head temperatures of +20°F and +160°F).

Neither of the materials are suitable for use as spacers in the current composite seal design. Zircoa "C" (Modified) spacers would result in seal thermal resistance of about 3.6 Hr-°F/BTU. Zircoa 1027 (Modified) spacers would yield a seal resistance of about 2.8 Hr-°F/BTU.

Appendix A presents the raw test data and Appendix B contains the thermal resistance calculations which were made.

Reference:

1. Second Quarter Report, Apollo Service Module Reaction Control System Engine Injector Chamber Seal Study - PR3008-2Q, dated February 1966.

CYLINDER INSTALLATION SKETCH

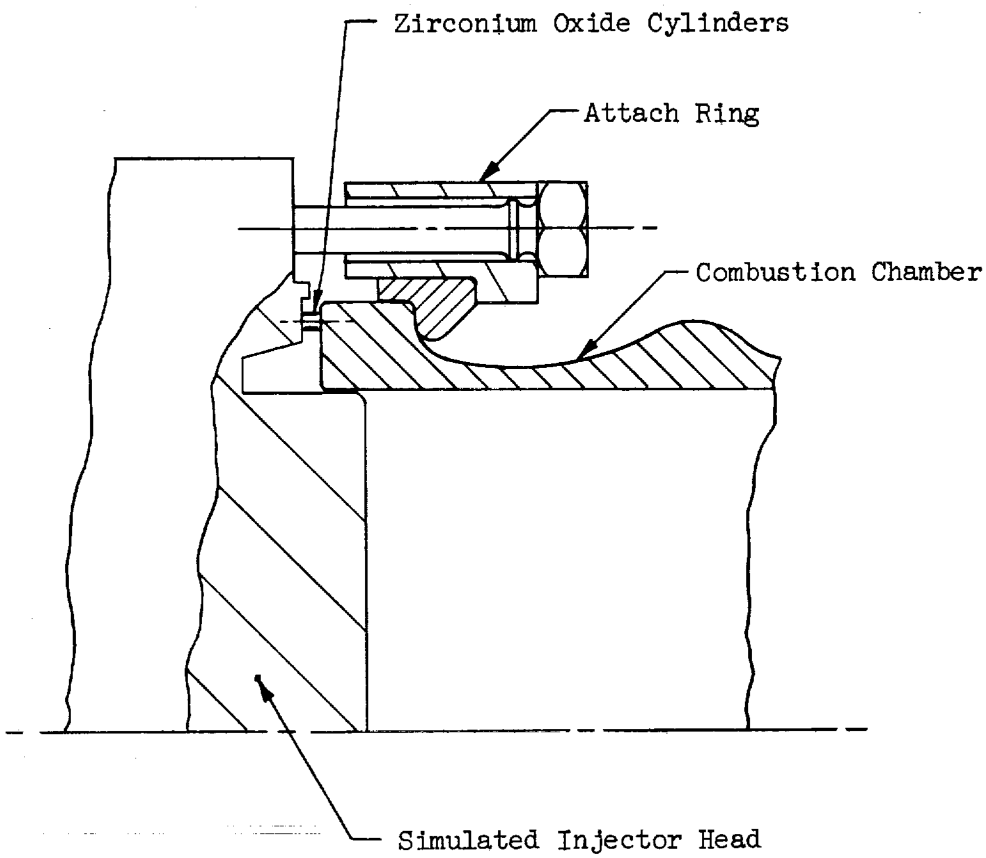

FIGURE 1

FIGURE 2

NEG. T11267-3

SCHEMATIC OF INSTRUMENTATION

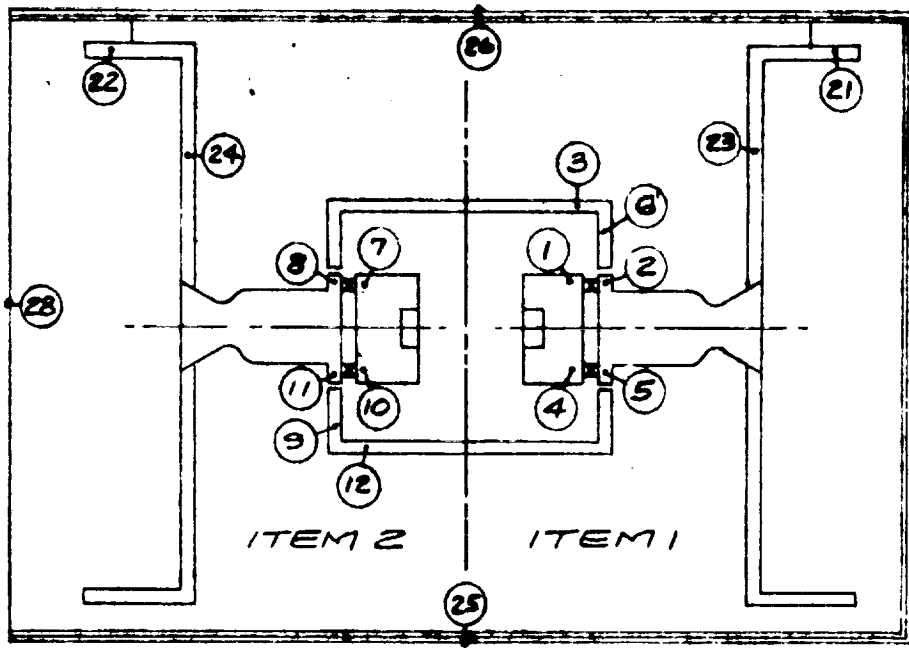

T/C NO.	LOCATION	ITEM	TYPE
1	INJ. HD. ADJACENT TO SEAL	1	I/C
2	COMBUSTOR FLANGE OPPOSITE T/C 1	1	I/C
3	TOP OF BOUNDARY FIXTURE	1	I/C
4	INJ. HD ADJACENT TO SEAL (180° OPP. T/C 1)	1	I/C
5	COMBUSTOR FLANGE OPPOSITE T/C 4	1	I/C
6	END OF BOUNDARY FIXTURE OPP. T/C 3	1	I/C
7	INJ. HD. ADJACENT TO SEAL	2	I/C
8	COMBUSTOR FLANGE OPPOSITE T/C 7	2	I/C
9	END OF BOUNDARY FIXTURE	2	I/C
10	INJ. HD. ADJACENT TO SEAL (180° OPP. T/C 7)	2	I/C
11	COMBUSTOR FLANGE OPPOSITE T/C 10	2	I/C
12	BOTTOM OF BOUNDARY FIXTURE OPP. T/C 9	2	I/C
13			
14			
15			
16			
17			
18			
19			
20			
21	TOP OF RADIATOR	1	C/A
22	TOP OF RADIATOR	2	C/A
23	WALL OF RADIATOR	1	C/A
24	WALL OF RADIATOR	2	C/A
25	BOTTOM OF LN_2 COOLED WALL	-	C/A
26	TOP " " " "	-	C/A
27	END " " " "	-	C/A
28	UNCOOLED WALL	-	C/A

APPENDIX A

TEST DATA

SEAL THERMAL RESISTANCE TEST
SIMULATED ENGINE
PER MTP 0041 APPENDIX B
TEST #5 DATE 3-31-66
4-1-66

ENG #1
SEAL TYPE ZIRCOA #1027
MODIFIED
60 EA CYLINDERS ONLY

ENG #2
SEAL TYPE ZIRCOA "C"
MODIFIED
60 EA CYLINDERS ONLY

DATA PT. No.	TIME	V.B.S. VOLTS	V.B.S. AMPS	VACUUM PRESS MM Hg	FACILITY TEMP T_{25}	T_{26}	T_{27}	T_{28}	ENG #1 HEAD HTR. VOLTS	M.A.	ENGINE TEMP. T_1	T_2	T_3	T_4	T_5	T_6	T_{21}	T_{23}	ENG #2 HEAD HTR. VOLTS	M.A.	ENGINE TEMP. T_7	T_8	T_9	T_{10}	T_{11}	T_{12}	T_{22}	T_{24}
1	2200	16.0	1.3	$.04\times10^{-4}$	-350	-350	-320	-75	20.0	212.0	+19	-28	+21	+20	-27	—	-63	-62	18.0	195.0	+20	-35	+22	+20	-35	+20	-60	-60
2	22:15	0	0	$.04\times10^{-4}$	-350	-350	-330	-96	20.0	212.0	+20	-28	+24	+20	-27	—	-63	-61	18.0	195.0	+20	-34	+23	+20	-35	+21	-60	-60
3	22:30	0	0	$.04\times10^{-4}$	-350	-350	-335	-96	20.0	212.0	+20	-28	+22	+20	-27	—	-63	-62	18.0	195.0	+20	-35	+21	+20	-34	+19	-60	-60
4	22:45	30.0	2.3	$.04\times10^{-4}$	-350	-350	-335	-96	20.0	212.0	+20	-28	+20	+20	-27	—	-63	-62	18.0	195.0	+20	-35	+19	+19	-35	+18	-61	-60
5	23:00	0	0	$.04\times10^{-4}$	-350	-350	-330	-96	20.0	212.0	+20	-27	+22	+20	-27	—	-63	-62	18.0	195.0	+20	-34	+22	+20	-35	+20	-61	-60
6	23:15	0	0	$.05\times10^{-4}$	-350	-350	-335	-96	20.0	212.0	+20	-27	+21	+21	-27	—	-63	-62	18.2	195.0	+20	-35	+20	+20	-34	+18	-61	-60
7	03:30	15.0	1.5	$.05\times10^{-4}$	-325	-325	-315	-90	31.5	300	+162	+55	+164	+162	+59	—	-24	-22	28.5	285	+160	+36	+163	+160	+35	+160	-25	-23
8	03:45	17.5	1.95	$.05\times10^{-4}$	-325	-325	-320	-90	31.5	305	+160	—	+160	+160	+59	—	-22	-20	28.5	285	+159	+36	+159	+159	+36	+156	-24	-22
9	04:00	30.0	2.2	$.05\times10^{-4}$	-325	-325	-305	-90	31.5	305	+160	—	+160	+160	+60	—	-20	-18	28.5	285	+158	+37	+159	+158	+37	+157	-22	-18
10	04:15	11.0	1.0	$.05\times10^{-4}$	-325	-325	-310	-89	31.5	305	+160	—	+161	+160	+60	—	-18	-16	28.5	285	+158	+40	+160	+158	+38	+157	-20	-17
11	04:30	39.0	2.9	$.07\times10^{-4}$	-325	-325	-305	-88	31.5	305	+160	—	+157	+160	+61	—	-17	-15	28.5	285	+158	+38	+156	+157	+39	+154	-19	-16
12	04:45	0.0	0.0	$.09\times10^{-4}$	-325	-325	-300	-88	31.5	305	+161	—	+154	+162	+62	—	-15	-13	28.5	285	+158	+46	+162	+158	+40	+160	-17	-15

APPENDIX B

CALCULATIONS

SEAL TEST #5 — 4-1-66

	ENG #1 ZIRCOA #1027 MODIFIED 60 EA CYL ONLY							ENG #2 ZIRCOA "C" MODIFIED 60 EA CYL ONLY						
DAY / TIME	T_W F°	T_C F°	ΔT F°	Q BTU/HR	R_J HR-°F/BTU	R_S HR-°F/BTU	T_S °F	T_W F°	T_C F°	ΔT °F	Q BTU/HR	R_J HR-°F/BTU	R_S HR-°F/BTU	T_S °F
7 / 0330	+162	+59	103	32.76	3.15	3.39		+160	+35	125	27.8	4.5	5.03	
8 / [illegible]	+160	+59	101	32.76	3.09	3.34		+159	+36	123	27.8	4.43	4.94	
9 / 0400	+160	+60	100	32.76	3.06	3.30		+158	+37	121	27.8	4.35	4.86	
10 / 0415	+160	+60	100	32.76	3.06	3.30		+158	+38	120	27.8	4.32	4.83	
11 / [illegible]	+160	+61	99	32.76	3.02	3.25		+157	+39	116	27.8	4.17	4.75	
12 / 0445	+162	+62	100	32.76	3.06	3.30		+158	+40	118	27.8	4.25	4.72	

SEAL TEST TEST #5 3-31-66 4-1-66

ENG #1 ZIRCOA #1027 MODIFIED 60 FA CYL. ONLY

ENG #2 ZIRCOA "C" MODIFIED 60 CYL. ONLY

RUN / DATA PT	ENG #1 T_H (T_4) °F	T_C (T_5) °F	ΔT °F	Q BTU/HR	R_J HR-°F/BTU	R_S HR-°F/BTU	T_S °F	ENG #2 T_H (T_{10}) °F	T_C (T_{11}) °F	ΔT °F	Q BTU/HR	R_J HR-°F/BTU	R_S HR-°F/BTU	T_S °F
1 / 22:00	+20	-27	47	14.45	3.24	3.6		20	-35	55	12.1	4.55	5.1	
2 / 22:15	+20	-27	47	14.45	3.24	3.6		20	-35	55	12.1	4.55	5.1	
3 / 22:30	+20	-27	47	14.45	3.24	3.6		20	-34	54	12.1	4.47	5.0	
4 / 22:45	+20	-27	47	14.45	3.24	3.6		19	-35	54	12.1	4.47	5.0	
5 / 23:00	+20	-27	47	14.45	3.24	3.6		20	-35	55	12.1	4.55	5.1	
6 / 23:15	+21	-27	47	14.45	3.33	3.61		20	-34	54	12.1	4.47	5.0	